Coral reef carbonate budgets and ecological drivers in the naturally high temperature and high alkalinity environment of the Red Sea

Anna Roik[1], Till Röthig[1], Claudia Pogoreutz[1], Christian R. Voolstra[1,*]

[1]Red Sea Research Center, King Abdullah University of Science and Technology, Thuwal, Saudi Arabia

*Corresponding author

Short title: Red Sea coral reef carbonate budget

Keywords: diel pH - total alkalinity - Red Sea - coral reef accretion - calcification - bioerosion - inorganic nutrients - environmental drivers

Abstract

The coral structural framework is crucial for maintaining reef ecosystem function and services. In the central Red Sea, a naturally high alkalinity is beneficial to reef growth, but rising water temperatures impair the calcification capacity of reef-building organisms. However, it is currently unknown how beneficial and detrimental factors affect the balance between calcification and erosion, and thereby the overall growth of the reef framework. To provide insight into present-day carbonate budgets and reef growth dynamics in the central Red Sea, we measured *in situ* net-accretion and net-erosion rates (G_{net}) by deployment of limestone blocks and estimated census-based carbonate budgets (G_{budget}) in four reef sites along a cross-shelf gradient (25 km). We assessed abiotic variables (i.e., temperature, inorganic nutrients, and carbonate system variables) and biotic drivers (i.e., calcifier and bioeroder abundances). On average, total alkalinity A_T (2346 – 2431 µmol kg^{-1}), aragonite saturation state (4.5 - 5.2 Ω_a), and pCO_2 (283 -315 µatm) were close to estimates of pre-industrial global ocean surface waters. Despite these calcification-favorable carbonate system conditions, G_{net} and G_{budget} encompassed positive (offshore) and negative net-production (midshore-lagoon and exposed nearshore site) estimates. Notably, G_{budget} maxima were lower compared to reef growth from pristine Indian Ocean sites. Yet, a comparison with historical data from the northern Red Sea suggests that overall reef growth in the Red Sea has likely remained similar since 1995. When assessing sites across the shelf gradient, A_T correlated well with reef growth rates ($\rho = 0.89$), while temperature was a weaker, negative correlate ($\rho = -0.71$). Further, A_T explained about 65 % of G_{budget} in a best fitting distance-based linear model. Interestingly, parrotfish abundances added up to 82% of explained variation, further substantiating recent studies highlighting the importance of parrotfish to reef ecosystem function. Our study provides a baseline that will be particularly useful in assessing future trajectories of reef growth capacities in the Red Sea under continuous ocean warming and acidification.

Introduction

Coral reef growth is limited to warm, aragonite-saturated, and oligotrophic tropical oceans and is pivotal for coral reef functioning (Buddemeier, 1997; Kleypas et al., 1999). The coral reef framework not only maintains a remarkable biodiversity, but also provides highly valuable ecosystem services that include food supply and coastal protection, among others (Moberg and Folke, 1999; Reaka-Kudla, 1997). Biogenic calcification, erosion, and dissolution cumulatively contribute to the formation of the reef framework constructed of calcium carbonate (CaCO3, mainly aragonite) (Glynn, 1997; Perry et al., 2008). The balance of carbonate loss and accretion are controlled by abiotic and biotic factors: temperature, properties of carbonate chemistry (e.g. pH, total alkalinity A_T, and aragonite saturation state Ω_a), calcifying benthic communities (scleractinian corals and coralline algal crusts), as well as grazing and endolithic bioeroders (e.g. parrotfish, sea urchins, and boring sponges) (Glynn and Manzello, 2015; Kleypas et al., 2001).

Positive carbonate budgets (G_{budget}) are maintained when reef calcification produces more $CaCO_3$ than is being removed, and rely in a great part on the ability of benthic calcifiers to precipitate calcium carbonate from seawater ($Ca^{2+} + CO_3^{2-} \leftrightarrow CaCO_3$, Tambutté et al. 2011). Calcification rates increase with higher temperature, but have an upper thermal limit (Jokiel and Coles, 1990; Marshall and Clode, 2004). In addition, A_T and $\Omega_{a,}$ are measures for the availability of the carbonate ions in seawater and their tendency to precipitate. Both positively correlate with calcification rates (Marubini et al., 2008; Schneider and Erez, 2006). Today's oceans are warming, which poses a potential threat to calcifying reef organisms, as high temperatures begin to exceed the thermal optima of calcifying organisms and thereby slowing down calcification (Carricart-Ganivet et al., 2012; Death et al., 2009). Simultaneously, as ocean acidification is commonly manifested in a decrease in ocean's pH and hence a decrease of Ω_a (Orr et al., 2005), calcification becomes energetically more costly (Cai et al., 2016; Cohen and Holcomb, 2009; Waldbusser et al., 2016). Finally, ocean acidification stimulates destructive processes, e.g. the proliferation and erosive activity of endolithic organisms that counteract reef growth (Enochs, 2015; Fang et al., 2013; Tribollet et al., 2009). A low or negative G_{budget} is generally associated with a disturbance of abiotic conditions that naturally have supported coral reef growth over the past millennia, i.e. specific temperature range, nutrient level, pH, and Ω_a (Buddemeier, 1997;

Kleypas et al., 1999). Today, in most tropical coral reefs, negative G_{budget} are a hallmark of reef degradation due to an increased intensity or frequency of extreme climate events (Eakin, 2001; Schuhmacher et al., 2005) or local human impacts, such as pollution and eutrophication (Chazottes et al., 2002; Edinger et al., 2000).

A census-based G_{budget} approach is a powerful tool to assess reef persistence of the reef framework allowing for a regional and global comparison of coral reef ecosystems (Kennedy et al., 2013; Perry et al., 2012, 2015). In more recent years, G_{budget} studies revealed that coral reef growth in the Caribbean has decreased by 50%, compared to historical mid- to late-Holocene reef growth. Also, 37% of all reefs studied are reported to be in a net-erosional state (Perry et al., 2013). In the Red Sea, coral reefs are exposed to challenging conditions in terms of high temperature and salinity regimes (Kleypas et al., 1999). Despite its high temperature and high salinity conditions (Roik et al., 2016), the Red Sea supports remarkable reef ecosystems with a coral reef framework along its entire coastline (Riegl et al., 2012). But coral core samples indicate that calcification rates have already been declining over the past decades worldwide, at the Great Barrier reef, the Caribbean, and also the central Red Sea. This decline in coral growth is widely attributed to ocean warming (Bak et al., 2009; Cantin et al., 2010; Cooper et al., 2008). In the central and southern Red Sea, present-day data show reduced calcification rates of corals and calcifying crusts when temperatures peak during summer (Roik et al., 2015; Sawall et al., 2015). While increasing temperatures are seemingly stressful and energetically demanding for calcifiers, high A_T values (~ 2400 μmol kg^{-1}, Metzl et al. 1989) in the Red Sea are putatively beneficial for carbonate accretion (Tambutté et al., 2011).

It is yet unknown how these present-day stressors and positive drivers of reef growth influence the overall reef net-carbonate production in this region. Availability of G_{budget} data for Red Sea coral reefs is poor (Jones et al., 2015). Aside from one early census-based assessment of the G_{budget} for a high-latitude reef in the Gulf of Aqaba (northern Red Sea), which considered both calcification and erosion/dissolution rates (Dullo et al., 1996), the remaining studies report calcification rates only (Cantin et al., 2010; Heiss, 1995; Roik et al., 2015; Sawall and Al-Sofyani, 2015). In this study we therefore set out to assess abiotic and biotic drivers of reef growth, and to determine the G_{budget} for coral reefs of the central Red Sea. First, to reveal the

present-day carbonate chemistry in the region, we examined sites along an environmental cross-shelf gradient during winter and summer. Second, we followed the census-based *ReefBudget* approach (Perry et al., 2012) to estimate net carbonate production states (G_{budget}) using reef site-specific biotic parameters. To achieve this, we assessed the abundances and calcification rates of the major reef-building coral taxa (*Porites*, *Pocillopora*, and *Acropora*) and calcareous crusts, along with the abundances and erosion rates of external macro bioeroders (parrotfish and sea urchins). Also, we measured net-accretion/erosion rates (G_{net}) *in situ* using limestone blocks deployed in the reefs, which additionally capture endolithic erosion rates. Finally, we explore the correlations of potential drivers on G_{net} and the overall $G_{budgets}$ using the abiotic and biotic data. Our study provides insight into reef growth dynamics and a comparative baseline to assess the effects of ongoing environmental change on reef growth in the central Red Sea.

Materials and Methods

Study sites and environmental monitoring

Study sites were located in the Saudi Arabian central Red Sea along an environmental cross-shelf gradient, which was previously described in (Roik et al., 2016) and Roik et al. (2015). Briefly, along this gradient dissolved oxygen increases, but chlorophyll-a, turbidity, and sedimentation decrease from nearshore to offshore, and are subject to seasonal variation (Roik et al., 2016). Data for this study were collected at four sites: an offshore forereef at ~25 km distance from the coastline (22° 20.456 N, 38° 51.127 E, "Shi'b Nazar"), two midshore sites (forereef and lagoon) at ~10 km distance (22° 15.100 N, 38° 57.386 E, "Al Fahal"), and a nearshore forereef at ~3km distance (22° 13.974 N, 39° 01.760 E, "Inner Fsar"). All sampling stations were located between 7.5 and 9 m depth. In the following, reef sites are referred to as "offshore", "midshore", "midshore lagoon", and "nearshore", respectively. Abiotic variables were measured in the study sites during two seasons in 2014. Temperature and pH were measured continuously recorded during "winter" (10^{th} February – 6^{th} April 2014) and "summer" (20^{th} June – 20^{th} September 2014) (see Roik et al., 2016). Additionally, for 5 – 6 consecutive weeks during each of the seasons, seawater samples were collected on SCUBA at the stations for the determination of inorganic nutrients and carbonate chemistry: nitrate and nitrite (NO_3^-&NO_2^-), ammonia (NH_4^+), phosphate (PO_4^{3-}), total alkalinity (A_T), and pH (Table S1).

Abiotic parameters - Continuous data

Conductivity-Temperature-Depth loggers (CTDs, SBE 16plusV2 SEACAT, RS-232, Sea-Bird Electronics, Bellevue, WA, USA) equipped with pH probes (SBE 18/27, Sea-Bird) were deployed at 0.5 m above the reef to collect times series data of temperature and pH_{CTD} at hourly intervals. Both sensors were factory-calibrated. To control for drift, pH probes were tested before and after deployment using certified standard buffers (pH-7 "38746" and pH-10 "38749", Fluka Analytics, Sigma-Aldrich, Germany). Data corrections were applied if necessary.

Abiotic parameters - Seawater samples

Seawater samples were collected on SCUBA at each of the stations using 4 L cubitainers (Table S1). Simultaneously, 60 mL seawater samples were taken over a 0.45 µm syringe filter for A_T

144 measurements. Immediately after sampling, the pH of the seawater (pH_{SWS}) was measured in
145 subsamples using a portable pH probe with an integrated temperature sensor (n = 3, precision of
146 ± 0.05 pH units, Orion 4 Star Plus, Thermo Fisher Scientific, MA, USA). Before each sampling
147 day, the probe was calibrated using certified standard buffers (pH-4 "38743," pH-7 "38746" and
148 pH-10 "38749", Fluka Analytics, Sigma-Aldrich). Seawater samples for inorganic nutrient
149 analyses and A_T measurement were transported on ice in the dark and were processed on the
150 same day. Samples were filtered over GF/F filters (0.7 µm, Whatman, UK) and filtrates were
151 frozen at -20 °C until analysis. The inorganic nutrient content (NO_3^-&NO_2^-, NH_4^+, and PO_4^{3-})
152 was determined using standard colorimetric tests and a Quick-Chem 8000 AutoAnalyzer
153 (Zellweger Analysis, Inc.). A_T samples were analyzed within 2 – 4 h after collection using an
154 automated acidimetric titration system (Titrando 888, Metrohm AG, Switzerland). Gran-type
155 titrations were performed with a 0.01 M HCl certified standard solution (prepared from 0.1 HCl,
156 Fluka Analytics) at a precision of ± 9 µmol kg^{-1}.
157
158 **Abiotic parameters - Net-accretion/erosion rates in limestone blocks (G_{net})**
159 Net-accretion/erosion rates were assessed using a limestone block "assay". Blocks (100 x 100 x
160 21 mm, ρ = 2.3 kg L^{-1}, n = 4) were weighed before and after deployment on the reefs, where they
161 were exposed to the natural processes of calcification and erosion. Before weighing (Mettler
162 Toledo XS2002S, readability = 10 mg), blocks were autoclaved and dried for a week in a climate
163 chamber at 40°C (BINDER, Tuttlingen, Germany). Blocks were deployed for 6 months
164 (September 2012 - March 2013), and for 12 months (June 2013 - June 2014) at six sites,
165 including the four reef sites and the offshore and nearshore back reefs, and for 30 months
166 (January 2013 – June 2015) in the four reef sites. Upon recovery, blocks were treated with 10 %
167 bleach for 24 – 36 h to remove organic material. G_{net} were expressed as normalized differences
168 of pre-deployment and post-deployment weights (kg m^{-2} yr^{-1}).
169
170 **Biotic parameters - Benthic community composition**
171 To assess coral reef benthic calcifier and bioeroder communities as input data for the carbonate
172 budgets, we conducted *in situ* surveys on SCUBA along the cross shelf gradient at each of our
173 study sites.The community composition and coverage of coral reef calcifying groups across was
174 assessed during both sampling seasons on SCUBA. We surveyed benthic calcifiers and non-

calcifiers and categorized them as follows: % cover total hard coral, % hard coral morphs (branching, encrusting, massive, and platy/foliose), % major reef-building coral families (Poritidae, Acroporidae, and Pocilloporidae), % cover calcareous crusts, % cover algae & sponges). For a detailed description of the benthic surveys please refer to Roik et al. (2015). In addition, benthic rugosity was assessed using the *Tape and Chain Method* (Perry et al., 2012).

Biotic parameters - Bioeroder populations along the cross shelf gradient

We surveyed the populations for the two main groups of coral reef framework bioerorders, the parrotfishes (Scaridae) (Bellwood, 1995; Bruggemann et al., 1996) and sea urchins (Echinoidea) (Bak, 1994). Surveys were conducted on SCUBA in stationary plots and line transects respectively per site (n = 6 each). For details on the field surveys and data treatment for biomass conversion, refer to the supplementary materials (Text S1).

Biotic parameters - Reef carbonate budgets (G_{budget})

Reef carbonate budgets (G_{budget}, kg m^{-1} yr^{-1}) were estimated following the census-based *ReefBudget* approach (Perry et al., 2012) adjusted for the central Red Sea. Site-specific benthic calcification rates ($G_{benthos}$, kg m^{-1} yr^{-1}), net-accretion/erosion rates of hard substrate ($G_{netbenthos}$, kg m^{-1} yr^{-1}), and erosion rates of crucial macro bioeroders such as sea urchins (E_{echino}, kg m^{-1} yr^{-1}) and parrotfishes (E_{parrot} , kg m^{-1} yr^{-1}) were incorporated in the G_{budget} estimates (Fig. 1). A detailed account of calculations is provided in the supplementary materials (Text S1, Equation box S1-3).

Statistical analyses - Abiotic parameters

Continuous temperature and pH data were summarized as daily means, daily standard deviations (SD), and daily minima/maxima. Diel profiles were plotted per reef and season including smoothing polynomial regression lines fitted by *geom_smooth* in R package *ggplot2* (LOESS, span = 0.1). Data were additionally visualized in histograms using the function *stat_bin*, as implemented in the R package *ggplot2* (R Core Team, 2013; Wickham and Chang, 2015). Univariate 2-factorial permutational ANOVAs (PERMANOVAs, Primer-E V6) were used to test the factors "reef" (nearshore, midshore lagoon, midshore, and offshore) and "season" (winter and summer). PERMANOVAS were performed on Euclidian resemblance matrices calculated from $\log_2$ (x+1) transformed data (Anderson et al., 2008) and were based on 999 permutations of

residuals under a reduced model and type II partial sums of squares. Within each significant factor, pair-wise post-hoc tests followed.

Using A_T, pH_{SWS} (seawater samples), salinity, and temperature (from CTD), carbonate chemistry parameters were calculated using the R package *seacarb* (Gattuso et al., 2015). Carbonic acid dissociation constants were employed as recommended in Dickson et al. (2007): K1 & K2 (Lueker et al., 2000), Kf (Perez and Fraga, 1987), and Ks (Dickson, 1990). Then, inorganic nutrients (NO_3^-&NO_2^-, NH_4^+, and PO_4^{3-}) and carbonate system variables (pH_{SWS}, A_T, C_T, Ωa, HCO_3^-, CO_3^{2-}) were evaluated using multivariate PERMANOVAs followed by principal coordinate ordination (PCO) according to the continuous data test design. Multivariate 2-factorial PERMANOVAs on Euclidian resemblance matrices created from normalized data were run under same specifications as above. Next, univariate 2-factorial ANOVAs were employed to evaluate the parameters separately under the same test design. For this, inorganic nutrients and carbonate chemistry parameters were transformed (log_2 (x+1): pH_{SWS}, A_T, Ωa; square-root: C_T, CO_3^{2-}; box-cox: HCO_{3-}) to meet the assumptions of normality and homoscedascity.

Statistical analyses - Net-accretion/erosion rates and carbonate budgets

G_{net} data were tested for effects of the factors "reef" (nearshore, midshore, and offshore), "site exposure" (fore- and backreef), and "deployment time" (6, 12, and 30 months). Because of the incomplete design due to missing the nearshore and offshore backreef sites in the 30-months deployment, a univariate 3-factorial PERMANOVA was conducted using Euclidian distance matrix 999 permutations of residuals under a reduced model and type II partial sum of squares.

G_{budget} were tested for statistical differences between the four "reef sites" (nearshore, midshore lagoon, midshore, and offshore) using a 1-factorial ANOVA, after box-cox transforming the data to meet the assumptions. In parallel, biotic variables were tested using a 1-factorial ANOVA for square-root transformed $G_{benthos}$, and non-parametric Kruskal-Wallis tests for non-transformed $G_{netbenthos}$, E_{echino}, and E_{parrot}. Tukey's HSD post-hoc tests followed where applicable.

Statistical analyses - Abiotic-biotic correlations

To evaluate the relationship of abiotic and biotic predictors of G_{net} and G_{budget}, a multivariate statistics approach was applied. Distance-based linear models (DistLM) were performed

237 including biotic and abiotic predictor variables (Primer-E V6). Models were tested for (a) G_{net}
238 and (b) G_{budget} data. G_{net} encompassed data of pooled 12- and 30-months measurements from
239 four reef sites (nearshore, midshore lagoon, midshore, and offshore). Predictor variables in (a)
240 were reef growth relevant abiotic parameters, comprising means and SDs from continuous
241 measurements of temperature and pH_{CTD} per reef site, and the means of inorganic nutrients (NO_3^-
242 &NO_2^-, NH_4^+, and PO_4^3) and carbonate chemistry parameters (A_T, C_T, Ω_a, HCO_{3-} , and CO_3^2)
243 (Table 1). Biotic variables that can potentially influence G_{net} on limestone blocks were added to
244 the models, i.e. parrotfish abundances and percentage cover (%) of calcareous crusts, both
245 derived from the reef surveys. In (b), the same predictor variables were employed as for (a), but
246 biotic predictors were extended with additional variables available from reef surveys i.e. % cover
247 total hard coral, % hard coral morphs (branching, encrusting, massive, and platy/foliose), %
248 major reef-building coral families (Poritidae, Acroporidae, and Pocilloporidae), % cover
249 calcareous crusts, % cover algae & sponges, benthic rugosity, and abundances of sea urchins and
250 parrotfish. Prior to DistLM, some predictor variables (i.e. sea urchin and parrotfish abundances,
251 % platy/foliose corals, and % Poritidae) were $\log_{10}$ (x+1) transformed to improve the symmetry
252 in their distributions following (Anderson et al., 2008). Both DistLM routines were performed on
253 Euclidian resemblance matrices, implementing the step-wise forward procedure with 9999
254 permutations and adjusted R^2 criterion. Additionally, Spearman rank correlation coefficients
255 were obtained for the response variables and their predictors.

Results

Abiotic parameters relevant for reef growth - Temperature and pH

The seasonal mean temperature varied between 26.0 ± 0.6°C in winter and 30.9 ± 0.7°C in summer across all reefs (Table 1). The difference across the shelf was on the average ~0.4°C (Table S9). The nearshore and midshore reef experienced the lowest (both ~26°C in winter), and the nearshore reef the highest mean temperatures (31.5 ± 0.6°C in summer). Seasonal and spatial differences in all temperature data (daily means, daily SDs, daily minima and maxima) were significant (Fig. 2 A-B, Table S10). Compared to all other sites, the nearshore reef experienced significantly higher daily maxima during summer ("daily max.", $p = 0.01$, Fig. 2 B, Table S9), and significantly lower minima during winter ($p < 0.01$, see also Table S10).

Across all reef sites, seasonal means for pH were 8.13 ± 0.19 in winter and 8.15 ± 0.13 in summer (Table 1). Lowest seasonal means were recorded on the midshore lagoon with 8.00 ± 0.17 in winter and 8.09 ± 0.22 in summer, and highest in the nearshore reef (8.25 ± 0.27 in winter and 8.31 ± 0.12 in summer). pH was intermediate on the exposed midshore and offshore (8.10 ± 0.05 to 8.16 ± 0.09). Overall, continuous pH data showed that spatial differences were more pronounced (with a mean difference between site averages of 0.15 pH units, Table S9), compared to minor effect of seasonality (with a mean difference between seasonal averages of 0.02 pH units). All daily-pH variables differed between reef sites ($p < 0.01$, Table S10, Fig. 2 C-D). Daily-pH SDs and maxima were significantly different between the seasons ($p < 0.01$ and $p < 0.05$, respectively). On all sites, pH followed a diel pattern with peak values around noon (12:00 h).

Abiotic parameters relevant for reef growth - Inorganic nutrients and carbonate chemistry

Inorganic nutrients and carbonate chemistry showed a major variation between the seasons (both $p < 0.001$, Table S10, Fig. S1). Specifically, NO_3^-&NO_2^- and NH_4^+ levels almost doubled in winter (0.36 ± 0.25 µmol L^{-1} and 0.35 ± 0.20 µmol L^{-1}) compared to summer (0.61 ± 0.25 µmol L^{-1} and 0.50 ± 0.22 µmol L^{-1}). In contrast, PO_4^{3-} was higher in winter than in summer (0.07 ± 0.02 vs. 0.03 ± 0.02 µmol L^{-1}, Table 1, Table S10 and Fig. 3 A). Highest inorganic nutrient contents were measured in the midshore lagoon with up to 0.68 µmol NO_3^-&NO_2^- L^{-1}, 0.58 µmol

287 NH_4^+ L^{-1} in summer, and 0.07 µmol PO_4^{3-} L^{-1} in winter, but PO_4^{3-} was also highe on the offshore
288 reef during winter (0.08 µmol $PO_4^{3-}L^{-1}$).
289
290 Carbonate chemistry analysis show overall elevated A_T, C_T and HCO_3^- concentrations in winter
291 (2423 ± 18 µmol A_T L^{-1}, 1990 ± 21 µmol C_T L^{-1}, and 1683 ± 24 µmol HCO_3^- L^{-1}) compared to
292 summer (2369 ± 38 A_T µmol L^{-1}, 1910 ± 36 µmol C_T L^{-1}, and 1588 ± 41 µmol HCO_3^- L^{-1}, Table
293 1, Fig. 3 B, Table S10). Estimates of pCO_2 in this study ranged 285 - 315 µatm across reef and
294 seasons. C_T and HCO_3^- were significantly higher during winter at all sites ($p < 0.05$), while A_T
295 was only higher in the nearshore ($p < 0.05$), remaining at similar levels in the other sites.
296 Conversely, Ω_a and CO_3^{2-} were overall reduced during winter (winter: 4.62 ± 0.12 Ω_a and 299 ±
297 7 µmol CO_3^{2-} L^{-1}; summer: 4.95 ± 0.28 Ω_a and 314 ± 17 µmol CO_3^{2-} L^{-1}). Changes in Ω_a between
298 the seasons were only found in the offshore site ($p < 0.05$). By trend, A_T and Ω_a increased from
299 nearshore to offshore with average differences of 32 µmol kg^{-1} and Ω_a 0.2 (Table S9).
300
301 **Biotic parameters relevant for reef growth - Benthic community composition**
302 A detailed account of benthic community structure in the study sites is outlined in Roik et al.
303 (2015). In brief, a low percentage of live substrate (< 40 %) was characteristic of the sheltered
304 and lagoonal sites. In exposed sites (offshore and midshore) a community of calcifying
305 organisms took up to 48 % of benthos cover on average (hard corals and calcareous crusts).
306 Major reef-building corals were the genera *Acropora*, *Pocillopora*, and *Porites* constituting 32–
307 56 % of the total hard coral cover.
308
309 **Biotic parameters relevant for reef growth - Abundances and biomasses of macro**
310 **bioeroders**
311 A total of 718 parrotfishes and 110 sea urchins were observed in the present study. For sea
312 urchins, mean abundances and biomass estimates of 0.002 ± 0.004 – 0.014 ± 0.006 individuals
313 m^{-2} and 0.05 ± 0.04 – 1.43 ± 0.98 g m^{-2} were observed, respectively (Table S4). Parrotfish mean
314 abundances and biomass estimates ranged from 0.05 ± 0.01 – 0.17 ± 0.60 individuals m^{-2} and
315 19.54 ± 5.56 – 82.18 ± 46.67 g m^{-2}, respectively (Table S6). The highest abundances and
316 biomasses of both parrotfishes and sea urchins were observed at the exposed nearshore site.
317 Abundances and biomasses of these two bioeroding groups decreased towards the exposed

midshore site, and then increased again towards the exposed offshore site. The inshore sites along with the exposed midshore site exhibited the largest range of sea urchin size classes (from categories 1 or 2 to the largest size class 5), while at the exposed sites, only the two smallest size classes of sea urchins were recorded. The largest parrotfishes (category 5 parrotfish, i.e., > 45 cm – 69 cm fork length) were observed at the midshore sites and the sheltered offshore site. With the exception of the exposed midshore site, category 1 (5 – 14 cm) parrotfish were commonly observed at all sites. In contrast, no category 6 parrotfish (≥ 70 cm fork length) were observed during the surveys.

Net-accretion/erosion rates

Cumulative net-accretion/erosion rates G_{net} were measured in assays over 6, 12, 30 months in the reef sites along the cross-shelf gradient. Visible boring traces of endolithic worms or sponges were only found on the surfaces of blocks recovered after 12 and 30 months (Fig. 4 A - H). G_{net} based on the 30-months deployment of blocks ranged between -0.96 and 0.37 kg m^{-2} yr^{-1} (Table 2). G_{net} for 12 and 30-months blocks were negative on the nearshore reef (between -0.96 and -0.2 kg m^{-2} yr^{-1}, i.e., net erosion is apparent), near-zero on the midshore reef (0.01 - 0.06 kg m^{-2} yr^{-1}, i.e., low net accretion), and positive on the offshore reef (up to 0.37 kg m^{-2} yr^{-1}, i.e., high net accretion). Reef sites and deployment times had a significant effect on the variability of G_{net} (Table S11). The rate of accretion/erosion was higher in the measurements over longest deployment period ($p < 0.001$, Figure S2).

Carbonate budgets

The carbonate budget G_{budget}, estimated via the *ReefBudget* approach (Perry et al., 2012) and averaged over all sites was 0.65 ± 1.73 kg m^{-2} yr^{-1}. This average encompasses values from the negative nearshore budget -1.48 ± 1.75 kg m^{-2} yr^{-1} to the positive offshore budget 2.44 ± 1.03 kg m^{-2} yr^{-1} (Table 3). G_{budget} significantly different between the reef sites ($p < 0.05$, Fig. 5 A), except for budgets in both midshore sites (lagoon and exposed), which were similar. Biotic variables that account for the carbonate budgets also differed by site, in the case of community calcification rates $G_{benthos}$ ($p < 0.05$, Fig. 5 B), and net-accretion/erosion of bare substrate $G_{netbenthos}$ ($p < 0.001$, Fig. 5 C). However, differences of parrot fish and echinoid erosion rates (E_{echino} and E_{parrot}) were not significant (Fig. 5 D -E).

349

350 **Abiotic and biotic drivers related to net-accretion rates and carbonate budgets**

351 Results from correlations and distance based linear models were similar for G_{net} and G_{budget}.
352 Temperature means, temperature SDs, and pH SDs were negatively correlated, while A_T, Ω_a,
353 CO_3^{2-}, and PO_4^{3-} were positively correlated with G_{net} ($\rho \geq |0.59|$, Table 4). The best model for
354 G_{net} data accounted for 56% (adjusted R^2) of the total variation. Here, A_T alone explained 54% of
355 the data and was the only statistically valid predictor of two abiotic variables in the model (the
356 second being Ω_a accounting for only 2% more, Table 5). Negative correlates of G_{budget} were
357 temperature means, temperature SDs, and pH SDs, while A_T, Ω_a, CO_3^{2-}, and PO_4^{3-} were positives
358 ($\rho \geq |0.59|$, Table 4). Among biotic variables, % total hard coral and calcareous crusts were
359 positively correlated. The best model for G_{budget} fitted six biotic and abiotic predictors and
360 explained total variation of 87% (adjusted R^2). Again, A_T was the major predictor explaining
361 65% alone. The biotic variable 'parrotfish abundance' added up to 85% of explained variation.
362 Both variables were significant in the test. The remaining four predictors included in the model
363 (NO_3^-&NO_2^-, % cover total hard coral, % encrusting coral, % of total hard coral, and %
364 Acroporidae) were non-significant and of minute relevance (altogether contributing only 3%,
365 Table 5).

Discussion

In this study we present environmental data of abiotic and biotic variables affecting present-day reef growth in the central Red Sea, a geographic region that is governed by unique conditions of high salinity and temperature, and that is impacted by ocean warming (Cantin et al., 2010; Raitsos et al., 2011). To date, reef growth, more specifically the calcification rates of reef-building corals in the Red Sea, have mostly been investigated regarding the effect of high temperature (Cantin et al., 2010; Roik et al., 2015; Sawall et al., 2015). Our study is therefore the first to link calcification data on an ecosystem scale with a range of abiotic and biotic variables (carbonate chemistry and nutrient availability; abundance and activity of main bioeroders, respectively). This is achieved by applying a census-based carbonate budget (G_{budget}) approach following (Perry et al., 2012). Our approach integrates the net-accretion/erosion rates (G_{net}) of six reef sites along the cross-shelf gradient assessed *in situ* using a limestone block assay. Additionally, our study provides an account of carbonate system conditions of the reefs in the central Red Sea, where such data is sparse. In the following, we discuss central Red Sea reef growth rates, which span from net-erosive states in the nearshore reef, to net-accretion in the midshore and offshore reefs, in the context of the prevailing abiotic and biotic drivers. Finally, we discuss our results in a global and historical context.

Abiotic factors governing reef growth in the central Red Sea

In this study we characterized the present-day abiotic conditions temperature, carbonate chemistry, and inorganic nutrients in the central Red Sea, which are considered environmental parameters that affect calcification and bioerosion on coral reefs. Notably, carbonate system variables, i.e., A_T, Ω_a, and pCO_2, observed in the study sites were on average closer to global pre-industrial values rather than to recent measurements from Pacific or Caribbean coral reef systems (Table 6). First, this comparison implies that Red Sea waters provide a beneficial environment for reef calcifiers that depend on availability of carbonate ions (i.e., high Ω_a, low pCO_2). Second, Red Sea waters have a high buffering capacity against ocean acidification and will probably protect reefs from this threat in the near future, while reefs outside the Red Sea might soon reach a critically low Ω_a threshold, which is projected to bring calcification to a halt (Manzello et al., 2008; Yeakel et al., 2015).

In the present study abiotic conditions varied on temporal (seasonal, diel) and spatial scales (cross-shelf gradient, exposed/sheltered reef sites). The observation of the seasonality of the carbonate system was similar to what we know about the high latitude reefs of the GoA, where A_T and C_T decrease while Ω_a increase during summer (Silverman et al., 2007a). While seasonal dynamics of inorganic nutrient concentrations have been shown by remote sensing data for the entire Red Sea basin (Raitsos et al., 2013), the present study demonstrates such dynamics on local reef scale, which again was similar to seasonality in the northern reefs of the GoA (Bednarz et al., 2015). Noteworthy for our study sites was a PO_4^{3-} enrichment during the winter.

Our continuous recordings show diel fluctuations of temperature and pH that are particularly strong in the nearshore and midshore lagoon sites. Diel pH fluctuation is the consequence of benthic biotic processes, i.e., calcification, dissolution, and respiration/photosynthesis that influence the balance of DIC species through removal, contribution, or exchange of molecules such as CO_3^{2-}, CO_2, and O_2, also referred to as biotic feedback (Bates et al., 2010; Silverman et al., 2007a; Zundelevich et al., 2007). The diel pH was more stable in the exposed midshore and offshore site reflecting a weaker biotic feedback, which was likely buffered by the higher rates of reef water mixing with the open sea water (Roik et al., 2016). Diel pH ranges measured on various coral reefs across the globe extend from ~7.80 to ~8.20 pH (Albright et al., 2013; Silbiger et al., 2014) and can span even larger ranges of up to ~1.40 pH units (Hofmann et al., 2011). Such diel pH variations suggest potential co-fluctuation of A_T and Ω_a, which can impact calcification rates at daily time scales. The nearshore and midshore lagoonal reefs from the present study offer suitable study sites to further investigate theses small-scale processes, which to date remain poorly studied.

The difference between nearshore to offshore A_T and Ω_a in our study area was on average at a range of 32 µmol A_T kg^{-1} and 0.2 Ω_a, respectively (Table S9). Similar cross-shelf differences are reported from e.g. reefs in Bermuda (20 – 40 µmol A_T kg^{-1} (Bates et al., 2010). Also in this case, water circulation patterns may explain these spatial gradients. The offshore and midshore reefs receive currents from the Red Sea basin (Roik et al., 2016), which supplies A_T saturated open sea water to the reefs. In contrast, the nearshore reef and midshore lagoon are mostly supplied by the

boundary current from the south (Roik et al., 2016) travelling along the coastal reef systems which deplete its A_T.

Indeed, the differences in seawater chemistry between offshore and nearshore reefs were correlated to reef growth processes: the most striking negative correlates were (a) mean temperatures and (b) pH variability, while (c) carbonate system parameters indicative of carbonate ion availability, i.e. A_T, Ω_a, CO_3^2, and also (d) PO_4^{3-} concentrations were positively related to reef growth. The negative correlates (a - b) reflect that higher mean temperatures and the impact of strong biotic feedbacks causing pH fluctuations govern nearshore habitats of low reef growth capacity. Previously, pH fluctuation on the micro-habitat scale has been shown to have a significant impact on accretion and erosion dynamics on coral reefs (Silbiger et al., 2014). Potentially these conditions physiologically challenge reef-building organisms exerting a negative effect on the reef growth rate. The positive effect of higher A_T, Ω_a, CO_3^{2-} on the calcification process is well established in laboratory experiments and on reef communities *in situ* (Langdon et al., 2000, Schneider and Erez, 2006, Silverman et al., 2007b, Bates et al., 2010). A_T was indeed the strongest predictor for both G_{net} and G_{budget}, alone explaining more than half of the variation in reef growth rates in the present study. Interestingly, our study also identifies PO_4^{3-} concentration, an essential macronutrient and important source of energy for primary producers and reef calcifiers (Ferrier-Pagès et al., 2016), to be a strong abiotic correlate of reef growth. While an overload of inorganic nutrients can be detrimental for the calcification process (Fabricius, 2005; Tambutté et al., 2011), our results show that in a highly oligotrophic reef system, such as the Red Sea, reef growth might be positively affected by seasonal increases in PO_4^{3-} levels. Experimental studies have shown that PO_4^{3-} additions can help maintain coral-algae symbiosis in reef-building corals that suffer from heat-stress (Ezzat et al., 2016). Also, under circumstances phosphorus limitation can increase the stress susceptibility of the coral-algae symbiosis (Pogoreutz et al., 2017; Rädecker et al., 2015; Wiedenmann et al., 2013). In the light of our results, it will be of interest to further study spatio-temporal variation of inorganic nutrient ratios to understand their effects on large-scale and long-term trends of reef growth in the central Red Sea.

458 **Biotic factors governing reef growth in the central Red Sea**

459 Calcifying benthic communities contribute to carbonate production and are considered the most
460 influential drivers for $G_{budgets}$ on global scale (Franco et al., 2016). Loss of coral cover rapidly
461 gives way to increased bioerosion as the critical force of degradation of the carbonate reef
462 framework. This has become particularly apparent in the Caribbean, where $G_{budgets}$ were reported
463 to shift into negative production states when live hard coral cover dropped below 10% (Perry et
464 al., 2013). Similarly, the relevance of benthic calcifying communities (coral and coralline algae)
465 was highly apparent in the present dataset from the central Red Sea: benthos cover percentage of
466 total hard coral and calcareous crusts constituted the strongest positive correlates for G_{budget}, and
467 the latter also for the variable G_{net}.
468
469 Considerably, the community composition and abundances of bioeroders potentially influence
470 reef carbonate budgets (Alvarez-Filip et al., 2009; Bak, 1994; Bellwood, 1995; Bronstein and
471 Loya, 2014; Bruggemann et al., 1996). Our analyses show that parrotfish erosion was a
472 considerable driving force across our study sites. Parrotfish abundances explained ~20% of
473 G_{budget} data variation, reflecting high parrotfish erosion in the nearshore likely contributing to the
474 net erosion state. Parrotfish abundances and biomasses were lowest at the sheltered midshore
475 site, and both increased towards inshore and offshore. Such differences can be attributed to
476 natural (e.g., species distribution, habitat preferences, reef rugosity) and/or anthropogenically-
477 driven factors (e.g., differential fishing pressure; McClanahan, 1994; McClanahan et al., 1994).
478 Indeed, the Saudi Arabian central Red Sea is subject to decade-long unregulated fishing pressure,
479 which has significantly altered overall reef fish community structures and reduced overall fish
480 biomass compared to less impacted regions in the Red Sea (Kattan et al., 2017). In undisturbed
481 coral reefs, parrotfishes are abundant herbivores with the differential capability to remove algal
482 turfs/macroalgae and/or coral reef framework and therefore a complex implications for coral reef
483 growth (Green and Bellwood, 2009): The ecological role of parrotfish grazing is the regulation
484 of benthic algal growth, supporting the recruitment of reef calcifiers and helping maintain a
485 coral-dominated state (Mumby, 2006). Hence, low parrotfish abundances would primarily reduce
486 erosion pressure on a reef, but secondarily promote phase-shift to non-calcifying organisms, such
487 as fleshy macroalgae (Hughes et al 2007). In the long term, this can cause a decrease in gross
488 carbonate production. Moreover, the overfishing of (parrot)fishes can reduce feeding pressure on

bioeroders or their larvae (e.g., sea urchins), resulting in an uncontrolled population increase leading reefs the trajectory of degradation driven by expanding bioeroder populations (Edgar et al., 2010; McClanahan and Shafir, 1990).

Cross-shelf patterns of net accretion/erosion rates and carbonate budget estimates

Net accretion/erosion rates (G_{net}) were measured in limestone block assays, in which blocks were exposed to natural levels of biotic $CaCO_3$ accretion (mainly by encrusting calcifiers), endolithic erosion by boring organisms, and surface abrasion by grazing fish along a cross-shelf gradient (Tribollet and Golubic, 2005). The resulting cumulative G_{net} reflects the colonization progress on the limestone blocks (Chazottes et al., 1995; Tribollet and Golubic, 2005). Differences in G_{net} along the cross-shelf gradient however were only observed after an exposure time of greater than 12 months, when well established epilithic and endolithic communities were apparent (Figure 4, Figure S2). Measurements from the 30-months assay reveal a net-erosion state (negative rates) in nearshore and net-accretion state (positive rates) in the offshore reef habitat. On average, G_{net} rates were in a similar range as observed in the reefs of Moorea (-0.49 - 0.63 kg m^{-2} yr^{-1}, (Pari et al., 1998). Yet, net-erosion states in the Red Sea did not reach the most extreme erosive scales reported from e.g. Moorea or the Andaman Sea, where lowest values were ~ - 7 to - 4 kg m^{-2} yr^{-1} (Pari et al., 1998; Schmidt and Richter, 2013).

$G_{budgets}$ represent the cumulative contribution of the major biotic drivers of reef growth ($G_{benthos}$, $G_{netbenthos}$, E_{echino} and E_{parrot}) for each site (Glynn, 1997; Perry et al., 2012) and resulted in a net-erosive budget in the nearshore reef, low net-accretion (near zero) in the midshore reef, up to a high net-accretion budget in offshore. Increasing across reef sites from nearshore to offshore, $G_{budgets}$ imply that nearshore reefs currently erode with half the speed that the offshore reefs grow, which may be interpreted as the formation of an offshore barrier reef in the central Red Sea (see Figure 5). The cross-shelf dynamics of $G_{budgets}$ and the biotic drivers (G and E) are complex and follow unique patterns that are in parts distinct from what we know from other reef systems. Other than observed in the GBR, where reef growth is reported to be high at inshore reefs (Browne et al., 2013), our nearshore study site, was net-erosive. Also, parrotfish erosion was highest in the nearshore area in the present Red Sea study, whereas lower rates were reported for the inshore reefs in the GBR (Hoey and Bellwood, 2007; Tribollet et al., 2002). On

Caribbean islands, parrotfish erosion rates are higher in leeward reefs (that are similar to protected nearshore habitats), but these sites are typically characterized by a high coral cover which drives a positive G_{budget} (Perry et al., 2012, 2014). Unlike in the Red Sea nearshore reef, which had the highest parrotfish erosion, but a negative G_{budget} due to low coral cover. This inter-regional comparison demonstrates that patterns encountered in one cross-shelf reef system should not necessarily be extrapolated to another system. In conclusion, *in situ* studies will be required for each unique system to understand its dynamics and its responses to environmental change.

Global and historical perspective on reef growth in the Red Sea

The central Red Sea $G_{budgets}$ are comparable with a majority of reef sites in the Caribbean, eastern and central western Pacific raning from -0.8 to 4.5 kg m^{-2} yr^{-1} (Mallela and Perry, 2007). The highest $G_{budgets}$ from the Red Sea are in the range of average global reef growth. However, Red Sea reefs do not reach highest accretion estimates reported, e.g, from the remote reefs in the Indian Ocean at the Chagos Archipelago which still hold the record with up to 9.8 kg m^{-2} yr^{-1} (Perry et al., 2015).

Due to lacking comparative data, it remains difficult to draw a historical perspective on $G_{budgets}$ in the Red Sea. Among the data available are pelagic and reefal net carbonate accretion rates, estimated using basin-scale historical measurements of A_T from 1998 (Steiner et al., 2014). Another data set is the census-based budget approach from a fringing reef in GoA from 1994 – 1996 ((Dullo et al., 1996). Both, the A_T-based reef accretion estimate from 1998 (0.9 kg $m^{-2}yr^{-1}$) and the GoA fringing reef budget from 1994 –1996 (0.7 – 0.9 kg $m^{-2}yr^{-1}$), constitute a good match. As well, $G_{budgets}$ assessed in the present study are in accordance with these historical data providing a comparison that supports the notion of stable reef growth rates in the Red Sea over the most recent decades. Additionally, the gross calcification rate of benthic communities ($G_{benthos}$) from our offshore site compares well with the maxima measured in GoA reefs in 1994 (2.7 kg m^{-2} yr^{-1}, Heiss, 1995).

Reef growth data from the Red Sea region is sparse, but suggest that coral reef growth might have not changed over the past 20 years despite the ongoing warming trend (Raitsos et al., 2011).

551 However, comparisons of data from the central Red Sea and GoA should be interpreted with
552 caution. Due to the strong latitudinal gradient of temperature and salinity between the central
553 Red Sea and GoA, reef growth dynamics from the two regions may differ and introduce bias in
554 the comparisons. Especially, in the light of a recent study demonstrating that increasing warming
555 rates of sea surface temperatures since 1990 coincided with decreasing coral calcification rates in
556 the central Red Sea (Cantin et al., 2010), it remains to be determined whether this declining
557 calcification capacity has an impact on the overall reef growth. In this context, the data presented
558 in this study will serve as a valuable baseline for comparative future studies in the central Red
559 Sea region. Importantly, these data were collected before the Third Global Bleaching Event,
560 which impacted the region during summer 2015 (Monroe et al., in review) and 2016. Hence, our
561 report will be of great value when assessing potential (long-term) changes in the Red Sea G_{budget}
562 after that significant disturbance.
563
564 **Conclusions**
565 The Red Sea represents a geographic region where coral reefs thrive under naturally high
566 temperature, high salinity, and high alkalinity conditions. Baseline data for reef growth from this
567 region are valuable as they provide insight into reef functioning under remarkably variable
568 abiotic conditions that deviate from the global average for coral reefs, and can potentially
569 provide a window into future ocean scenarios. Our data show that carbonate chemistry compares
570 to estimates of preindustrial global ocean surface water, suggesting low susceptibility to ocean
571 acidification for reef calcifiers in the Red Sea. Yet, it remains to be determined how small-scale
572 changes in carbonate chemistry will affect overall reef growth in the central Red Sea under
573 prevailing high temperatures. The offshore reef growth rate from the central Red Sea are
574 comparable to other regions of this world and historical Red Sea data suggest that rates might
575 have not decreased over the past few decades, but rather remained unchanged since 1995 in the
576 Red Sea. Our study shows that carbonate budgets are a powerful tool to track the trajectories of
577 modern-day and future reef states. Our data should provide a valuable baseline and foundation
578 data for evaluating the impact of disturbances, such as the most recent high temperature
579 anomalies on the reef-building communities and the overall reef growth capacity in the central
580 Red Sea.
581

582 **Acknowledgements**

583 We thank CMOR for assistance with field operations. This study was supported by funding from
584 King Abdullah University of Science and Technology (KAUST).

585

586 **References**

587

588 Albright, R., Langdon, C. and Anthony, K. R. N.: Dynamics of seawater carbonate chemistry,
589 production, and calcification of a coral reef flat, Central Great Barrier Reef, Biogeosciences
590 Discuss., 10, 7641–7676, doi:10.5194/bgd-10-7641-2013, 2013.

591 Alvarez-Filip, L., Dulvy, N. K., Gill, J. A., Côté, I. M. and Watkinson, A. R.: Flattening of
592 Caribbean coral reefs: region-wide declines in architectural complexity, Proc. R. Soc. Lond. B
593 Biol. Sci., 276(1669), 3019–3025, doi:10.1098/rspb.2009.0339, 2009.

594 Anderson, M. J., Gorley, R. N. and Clarke, K. R.: PERMANOVA+ for PRIMER: Guide to
595 software and statistical methods, 2008.

596 Bak, R. P. M.: Sea urchin bioerosion on coral reefs: place in the carbonate budget and relevant
597 variables, Coral Reefs, 13(2), 99–103, doi:10.1007/BF00300768, 1994.

598 Bak, R. P. M., Nieuwland, G. and Meesters, E. H.: Coral Growth Rates Revisited after 31 Years:
599 What is Causing Lower Extension Rates in Acropora Palmata?, Bull. Mar. Sci., 84(3), 287–294,
600 2009.

601 Bates, N. R., Amat, A. and Andersson, A. J.: Feedbacks and responses of coral calcification on
602 the Bermuda reef system to seasonal changes in biological processes and ocean acidification,
603 Biogeosciences, 7(8), 2509–2530, doi:10.5194/bg-7-2509-2010, 2010.

604 Bauman, A. G., Feary, D. A., Heron, S. F., Pratchett, M. S. and Burt, J. A.: Multiple
605 environmental factors influence the spatial distribution and structure of reef communities in the
606 northeastern Arabian Peninsula, Mar. Pollut. Bull., 72(2), 302–312,
607 doi:10.1016/j.marpolbul.2012.10.013, 2013.

608 Bednarz, V., Cardini, U., van Hoytema, N., Al-Rshaidat, M. and Wild, C.: Seasonal variation in
609 dinitrogen fixation and oxygen fluxes associated with two dominant zooxanthellate soft corals
610 from the northern Red Sea, Mar. Ecol. Prog. Ser., 519, 141–152, doi:10.3354/meps11091, 2015.

611 Bellwood, D. R.: Direct estimate of bioerosion by two parrotfish species, Chlorurus gibbus and
612 C. sordidus, on the Great Barrier Reef, Australia, Mar. Biol., 121(3), 419–429,
613 doi:10.1007/BF00349451, 1995.

614 Bronstein, O. and Loya, Y.: Echinoid community structure and rates of herbivory and bioerosion
615 on exposed and sheltered reefs, J. Exp. Mar. Biol. Ecol., 456, 8–17,
616 doi:10.1016/j.jembe.2014.03.003, 2014.

617 Browne, N. K., Smithers, S. G. and Perry, C. T.: Carbonate and terrigenous sediment budgets for
618 two inshore turbid reefs on the central Great Barrier Reef, Mar. Geol., 346, 101–123,
619 doi:10.1016/j.margeo.2013.08.011, 2013.

620 Bruggemann, J., van Kessel, A., van Rooij, J. and Breeman, A.: Bioerosion and sediment
621 ingestion by the Caribbean parrotfish Scarus vetula and Sparisoma viride: implications of fish

size, feeding mode and habitat use, Mar. Ecol. Prog. Ser., 134, 59–71, doi:10.3354/meps134059, 1996.

Buddemeier, R. W.: Symbiosis: Making light work of adaptation, Nature, 388(6639), 229–230, doi:10.1038/40755, 1997.

Cai, W.-J., Ma, Y., Hopkinson, B. M., Grottoli, A. G., Warner, M. E., Ding, Q., Hu, X., Yuan, X., Schoepf, V., Xu, H., Han, C., Melman, T. F., Hoadley, K. D., Pettay, D. T., Matsui, Y., Baumann, J. H., Levas, S., Ying, Y. and Wang, Y.: Microelectrode characterization of coral daytime interior pH and carbonate chemistry, Nat. Commun., 7, 11144, doi:10.1038/ncomms11144, 2016.

Cantin, N. E., Cohen, A. L., Karnauskas, K. B., Tarrant, A. M. and McCorkle, D. C.: Ocean Warming Slows Coral Growth in the Central Red Sea, Science, 329(5989), 322–325, doi:10.1126/science.1190182, 2010.

Carricart-Ganivet, J. P., Cabanillas-Terán, N., Cruz-Ortega, I. and Blanchon, P.: Sensitivity of Calcification to Thermal Stress Varies among Genera of Massive Reef-Building Corals, PLoS ONE, 7(3), e32859, doi:10.1371/journal.pone.0032859, 2012.

Chazottes, V., Campion-Alsumard, T. L. and Peyrot-Clausade, M.: Bioerosion rates on coral reefs: interactions between macroborers, microborers and grazers (Moorea, French Polynesia), Palaeogeogr. Palaeoclimatol. Palaeoecol., 113(2–4), 189–198, doi:10.1016/0031-0182(95)00043-L, 1995.

Chazottes, V., Le Campion-Alsumard, T., Peyrot-Clausade, M. and Cuet, P.: The effects of eutrophication-related alterations to coral reef communities on agents and rates of bioerosion (Reunion Island, Indian Ocean), Coral Reefs, 21(4), 375–390, 2002.

Cohen, A. L. and Holcomb, M.: Why corals care about ocean acidification: uncovering the mechanism, Oceanography, (22), 118–127, 2009.

Cooper, T. F., Death, G., Fabricius, K. E. and Lough, J. M.: Declining coral calcification in massive Porites in two nearshore regions of the northern Great Barrier Reef, Glob. Change Biol., 14(3), 529–538, doi:10.1111/j.1365-2486.2007.01520.x, 2008.

Couce, E., Ridgwell, A. and Hendy, E. J.: Environmental controls on the global distribution of shallow-water coral reefs, J. Biogeogr., 39(8), 1508–1523, doi:10.1111/j.1365-2699.2012.02706.x, 2012.

Death, G., Lough, J. M. and Fabricius, K. E.: Declining Coral Calcification on the Great Barrier Reef, Science, 323(5910), 116–119, doi:10.1126/science.1165283, 2009.

Dickson, A. G.: Standard potential of the reaction: AgCl(s) + 12H2(g) = Ag(s) + HCl(aq), and and the standard acidity constant of the ion HSO4− in synthetic sea water from 273.15 to 318.15 K, J. Chem. Thermodyn., 22(2), 113–127, doi:10.1016/0021-9614(90)90074-Z, 1990.

657 Dickson, A. G., Sabine, C. L. and Christian, J. R.: Guide to best practices for ocean CO2
658 measurements, PICES Spec. Publ., 3, pp 191, 2007.

659 Dullo, W.-C., Reijmer, J., Schuhmacher, H., Eisenhauer, A., Hassan, M. and Heiss, G.: Holocene
660 reef growth and recent carbonate production in the Red Sea, [online] Available from:
661 https://www.researchgate.net/publication/230751439_Holocene_reef_growth_and_recent_carbo
662 nate_production_in_the_Red_Sea, 1996.

663 Eakin, C. M.: A tale of two Enso Events: carbonate budgets and the influence of two warming
664 disturbances and intervening variability, Uva Island, Panama, Bull. Mar. Sci., 69(1), 171–186,
665 2001.

666 Edgar, G. J., Banks, S. A., Brandt, M., Bustamante, R. H., Chiriboga, A., Earle, S. A., Garske, L.
667 E., Glynn, P. W., Grove, J. S., Henderson, S., Hickman, C. P., Miller, K. A., Rivera, F. and
668 Wellington, G. M.: El Niño, grazers and fisheries interact to greatly elevate extinction risk for
669 Galapagos marine species, Glob. Change Biol., 16(10), 2876–2890, doi:10.1111/j.1365-
670 2486.2009.02117.x, 2010.

671 Edinger, E. N., Limmon, G. V., Jompa, J., Widjatmoko, W., Heikoop, J. M. and Risk, M. J.:
672 Normal coral growth rates on dying reefs: Are coral growth rates good indicators of reef health?,
673 Mar. Pollut. Bull., 40(5), 404–425, 2000.

674 Enochs, I. C.: Ocean acidification enhances the bioerosion of a common coral reef sponge:
675 implications for the persistence of the Florida Reef Tract, Bull. Mar. Sci., 91, 271–290,
676 doi:10.5343/bms.2014.1045, 2015.

677 Ezzat, L., Maguer, J.-F., Grover, R. and Ferrier-Pagès, C.: Limited phosphorus availability is the
678 Achilles heel of tropical reef corals in a warming ocean, Sci. Rep., 6, 31768,
679 doi:10.1038/srep31768, 2016.

680 Fabricius, K. E.: Effects of terrestrial runoff on the ecology of corals and coral reefs: review and
681 synthesis, Mar. Pollut. Bull., 50(2), 125–146, doi:10.1016/j.marpolbul.2004.11.028, 2005.

682 Fang, J. K. H., Mello-Athayde, M. A., Schönberg, C. H. L., Kline, D. I., Hoegh-Guldberg, O.
683 and Dove, S.: Sponge biomass and bioerosion rates increase under ocean warming and
684 acidification, Glob. Change Biol., 19(12), 3581–3591, doi:10.1111/gcb.12334, 2013.

685 Ferrier-Pagès, C., Godinot, C., D'Angelo, C., Wiedenmann, J. and Grover, R.: Phosphorus
686 metabolism of reef organisms with algal symbionts, Ecol. Monogr., 86(3), 262–277,
687 doi:10.1002/ecm.1217, 2016.

688 Franco, C., Hepburn, L. A., Smith, D. J., Nimrod, S. and Tucker, A.: A Bayesian Belief Network
689 to assess rate of changes in coral reef ecosystems, Environ. Model. Softw., 80, 132–142,
690 doi:10.1016/j.envsoft.2016.02.029, 2016.

691 Gattuso, J. P., Epitalon, J. M. and Lavigne: seacarb: seawater carbonate chemistry with R. R
692 package version 3.0. [online] Available from: http://CRAN.R-project.org/package=seacarb,
693 2015.

694 Glynn, P. W.: Bioerosion and coral-reef growth: a dynamic balance, in Life and Death of Coral
695 Reefs, edited by C. Birkeland, pp. 68–94, Chapman and Hall, Ney York, USA., 1997.

696 Glynn, P. W. and Manzello, D. P.: Bioerosion and Coral Reef Growth: A Dynamic Balance, in
697 Coral Reefs in the Anthropocene, edited by C. Birkeland, pp. 67–97, Springer Netherlands.,
698 2015.

699 Gray, S. E. C., DeGrandpre, M. D., Langdon, C. and Corredor, J. E.: Short-term and seasonal
700 pH, pCO2 and saturation state variability in a coral-reef ecosystem, Glob. Biogeochem. Cycles,
701 26(3), doi:10.1029/2011GB004114, 2012.

702 Green, A. L. and Bellwood, D. R.: Monitoring functional groups of herbivorous reef fishes as
703 indicators of coral reef resilience: a practical guide for coral reef managers in the Asia Pacific
704 region, International Union for Conservation of Nature, IUCN, Gland, Switzerland. [online]
705 Available from: ftp://ftp.library.noaa.gov/noaa_documents.lib/CoRIS/IUCN_herbivorous_reef-
706 fishes_2009.pdf (Accessed 30 September 2017), 2009.

707 Heiss, G. A.: Carbonate production by scleractinian corals at Aqaba, Gulf of Aqaba, Red Sea,
708 Facies, 33(1), 19–34, doi:10.1007/BF02537443, 1995.

709 Hoey, A. S. and Bellwood, D. R.: Cross-shelf variation in the role of parrotfishes on the Great
710 Barrier Reef, Coral Reefs, 27(1), 37–47, doi:10.1007/s00338-007-0287-x, 2007.

711 Hofmann, G. E., Smith, J. E., Johnson, K. S., Send, U., Levin, L. A., Micheli, F., Paytan, A.,
712 Price, N. N., Peterson, B., Takeshita, Y., Matson, P. G., Crook, E. D., Kroeker, K. J., Gambi, M.
713 C., Rivest, E. B., Frieder, C. A., Yu, P. C. and Martz, T. R.: High-Frequency Dynamics of Ocean
714 pH: A Multi-Ecosystem Comparison, edited by W.-C. Chin, PLoS ONE, 6(12), e28983,
715 doi:10.1371/journal.pone.0028983, 2011.

716 Jokiel, P. L. and Coles, S. L.: Response of Hawaiian and other Indo-Pacific reef corals to
717 elevated temperature, Coral Reefs, 8(4), 155–162, doi:10.1007/BF00265006, 1990.

718 Jones, N. S., Ridgwell, A. and Hendy, E. J.: Evaluation of coral reef carbonate production
719 models at a global scale, Biogeosciences, 12(5), 1339–1356, doi:10.5194/bg-12-1339-2015,
720 2015.

721 Kattan, A., Coker, D. J. and Berumen, M. L.: Reef fish communities in the central Red Sea show
722 evidence of asymmetrical fishing pressure, Mar. Biodivers., 1–12, doi:10.1007/s12526-017-
723 0665-8, 2017.

724 Kennedy, E. V., Perry, C. T., Halloran, P. R., Iglesias-Prieto, R., Schönberg, C. H. L., Wisshak,
725 M., Form, A. U., Carricart-Ganivet, J. P., Fine, M., Eakin, C. M. and Mumby, P. J.: Avoiding
726 Coral Reef Functional Collapse Requires Local and Global Action, Curr. Biol., 23(10), 912–918,
727 doi:10.1016/j.cub.2013.04.020, 2013.

728 Kleypas, J., Buddemeier, R. and Gattuso, J.-P.: The future of coral reefs in an age of global
729 change, Int. J. Earth Sci., 90(2), 426–437, doi:10.1007/s005310000125, 2001.

730 Kleypas, J. A., McManus, J. W. and Menez, L. A. B.: Environmental Limits to Coral Reef
731 Development: Where Do We Draw the Line?, Am. Zool., 39, 146–159, 1999.

732 Lueker, T. J., Dickson, A. G. and Keeling, C. D.: Ocean pCO2 calculated from dissolved
733 inorganic carbon, alkalinity, and equations for K1 and K2: validation based on laboratory
734 measurements of CO2 in gas and seawater at equilibrium, Mar. Chem., 70(1–3), 105–119,
735 doi:10.1016/S0304-4203(00)00022-0, 2000.

736 Mallela, J. and Perry, C.: Calcium carbonate budgets for two coral reefs affected by different
737 terrestrial runoff regimes, Rio Bueno, Jamaica, Coral Reefs, 26(1), 129–145,
738 doi:10.1007/s00338-006-0169-7, 2007.

739 Manzello, D. P.: Ocean acidification hotspots: Spatiotemporal dynamics of the seawater CO2
740 system of eastern Pacific coral reefs, Limnol. Oceanogr., 55(1), 239–248,
741 doi:10.4319/lo.2010.55.1.0239, 2010.

742 Manzello, D. P., Kleypas, J. A., Budd, D. A., Eakin, C. M., Glynn, P. W. and Langdon, C.:
743 Poorly cemented coral reefs of the eastern tropical Pacific: Possible insights into reef
744 development in a high-CO2 world, Proc. Natl. Acad. Sci., 105(30), 10450–10455, 2008.

745 Marshall, A. T. and Clode, P.: Calcification rate and the effect of temperature in a zooxanthellate
746 and an azooxanthellate scleractinian reef coral, Coral Reefs, 23(2), 218–224,
747 doi:10.1007/s00338-004-0369-y, 2004.

748 Marubini, F., Ferrier-Pagès, C., Furla, P. and Allemand, D.: Coral calcification responds to
749 seawater acidification: a working hypothesis towards a physiological mechanism, Coral Reefs,
750 27(3), 491–499, doi:10.1007/s00338-008-0375-6, 2008.

751 McClanahan, T. R.: Kenyan coral reef lagoon fish: effects of fishing, substrate complexity, and
752 sea urchins, Coral Reefs, 13(4), 231–241, doi:10.1007/BF00303637, 1994.

753 McClanahan, T. R. and Shafir, S. H.: Causes and consequences of sea urchin abundance and
754 diversity in Kenyan coral reef lagoons, Oecologia, 83(3), 362–370, doi:10.1007/BF00317561,
755 1990.

756 McClanahan, T. R., Nugues, M. and Mwachireya, S.: Fish and sea urchin herbivory and
757 competition in Kenyan coral reef lagoons: the role of reef management, J. Exp. Mar. Biol. Ecol.,
758 184(2), 237–254, doi:10.1016/0022-0981(94)90007-8, 1994.

759 Metzl, N., Moore, B., Papaud, A. and Poisson, A.: Transport and carbon exchanges in Red Sea
760 Inverse Methodology, Glob. Biogeochem. Cycles, 3(1), 1–26, doi:10.1029/GB003i001p00001,
761 1989.

762 Moberg, F. and Folke, C.: Ecological goods and services of coral reef ecosystems, Ecol. Econ.,
763 29, 215–233, 1999.

764 Monroe, A. A., Ziegler, M., Roik, A., Röthig, T., Hardenstin, R., Emms, M., Jensen, T.,
765 Voolstra, C. R. and Berumen, M. L.: In situ observations of coral bleaching in the central Saudi
766 Arabian Red Sea during the 2015/2016 global coral bleaching event, PLOS ONE in review.

767 Mumby, P. J.: The Impact Of Exploiting Grazers (Scaridae) On The Dynamics Of Caribbean
768 Coral Reefs, Ecol. Appl., 16(2), 747–769, doi:10.1890/1051-
769 0761(2006)016[0747:TIOEGS]2.0.CO;2, 2006.

770 Orr, J. C., Fabry, V. J., Aumont, O., Bopp, L., Doney, S. C., Feely, R. A., Gnanadesikan, A.,
771 Gruber, N., Ishida, A., Joos, F., Key, R. M., Lindsay, K., Maier-Reimer, E., Matear, R., Monfray,
772 P., Mouchet, A., Najjar, R. G., Plattner, G.-K., Rodgers, K. B., Sabine, C. L., Sarmiento, J. L.,
773 Schlitzer, R., Slater, R. D., Totterdell, I. J., Weirig, M.-F., Yamanaka, Y. and Yool, A.:
774 Anthropogenic ocean acidification over the twenty-first century and its impact on calcifying
775 organisms, Nature, 437(7059), 681–686, doi:10.1038/nature04095, 2005.

776 Pari, N., Peyrot-Clausade, M., Le Champion-Alsumard, T., Hutchings, P., Chazottes, V.,
777 Gobulic, S., Le Champion, J. and Fontaine, M. F.: Bioerosion of experimental substrates on high
778 islands and on atoll lagoons (French Polynesia) after two years of exposure, Mar. Ecol. Prog.
779 Ser., 166, 119–130, 1998.

780 Perez, F. F. and Fraga, F.: The pH measurements in seawater on the NBS scale, Mar. Chem.,
781 21(4), 315–327, doi:10.1016/0304-4203(87)90054-5, 1987.

782 Perry, C., Edinger, E., Kench, P., Murphy, G., Smithers, S., Steneck, R. and Mumby, P.:
783 Estimating rates of biologically driven coral reef framework production and erosion: a new
784 census-based carbonate budget methodology and applications to the reefs of Bonaire, Coral
785 Reefs, 31(3), 853–868, doi:10.1007/s00338-012-0901-4, 2012.

786 Perry, C. T. and Larcombe, P.: Marginal and non-reef-building coral environments, Coral Reefs,
787 22(4), 427–432, doi:10.1007/s00338-003-0330-5, 2003.

788 Perry, C. T., Spencer, T. and Kench, P. S.: Carbonate budgets and reef production states: a
789 geomorphic perspective on the ecological phase-shift concept, Coral Reefs, 27(4), 853–866,
790 doi:10.1007/s00338-008-0418-z, 2008.

791 Perry, C. T., Murphy, G. N., Kench, P. S., Smithers, S. G., Edinger, E. N., Steneck, R. S. and
792 Mumby, P. J.: Caribbean-wide decline in carbonate production threatens coral reef growth, Nat.
793 Commun., 4, 1402, doi:10.1038/ncomms2409, 2013.

794 Perry, C. T., Murphy, G. N., Kench, P. S., Edinger, E. N., Smithers, S. G., Steneck, R. S. and
795 Mumby, P. J.: Changing dynamics of Caribbean reef carbonate budgets: emergence of reef
796 bioeroders as critical controls on present and future reef growth potential, Proc. R. Soc. B Biol.
797 Sci., 281(1796), 20142018–20142018, doi:10.1098/rspb.2014.2018, 2014.

798 Perry, C. T., Murphy, G. N., Graham, N. A. J., Wilson, S. K., Januchowski-Hartley, F. A. and
799 East, H. K.: Remote coral reefs can sustain high growth potential and may match future sea-level
800 trends, Sci. Rep., 5, 18289, doi:10.1038/srep18289, 2015.

Pogoreutz, C., Rädecker, N., Cárdenas, A., Gärdes, A., Voolstra, C. R. and Wild, C.: Sugar enrichment provides evidence for a role of nitrogen fixation in coral bleaching, Glob. Change Biol., n/a-n/a, doi:10.1111/gcb.13695, 2017.

R Core Team: R: A language and environment for statistical computing, R Foundation for Statistical Computing, Vienna, Austria. [online] Available from: http://www.R-project.org/, 2013.

Rädecker, N., Pogoreutz, C., Voolstra, C. R., Wiedenmann, J. and Wild, C.: Nitrogen cycling in corals: the key to understanding holobiont functioning?, Trends Microbiol., doi:10.1016/j.tim.2015.03.008, 2015.

Raitsos, D. E., Hoteit, I., Prihartato, P. K., Chronis, T., Triantafyllou, G. and Abualnaja, Y.: Abrupt warming of the Red Sea, Geophys. Res. Lett., 38(14), L14601, doi:10.1029/2011GL047984, 2011.

Raitsos, D. E., Pradhan, Y., Brewin, R. J. W., Stenchikov, G. and Hoteit, I.: Remote Sensing the Phytoplankton Seasonal Succession of the Red Sea, PLoS ONE, 8(6), e64909, doi:10.1371/journal.pone.0064909, 2013.

Reaka-Kudla, M. L.: The Global Biodiversity of Coral Reefs: A Comparison with Rainforests, in Biodiversity II: Understanding and Protecting Our Biological Resources, edited by M. L. Reaka-Kudla, D. E. Wilson, and E. O. Wilson, pp. 83–106, The Joseph Henry Press, USA., 1997.

Riegl, B.: Climate change and coral reefs: different effects in two high-latitude areas (Arabian Gulf, South Africa), Coral Reefs, 22(4), 433–446, doi:10.1007/s00338-003-0335-0, 2003.

Riegl, B. M., Bruckner, A. W., Rowlands, G. P., Purkis, S. J. and Renaud, P.: Red Sea Coral Reef Trajectories over 2 Decades Suggest Increasing Community Homogenization and Decline in Coral Size, PLoS ONE, 7(5), e38396, doi:10.1371/journal.pone.0038396, 2012.

Roik, A., Roder, C., Röthig, T. and Voolstra, C. R.: Spatial and seasonal reef calcification in corals and calcareous crusts in the central Red Sea, Coral Reefs, 1–13, doi:10.1007/s00338-015-1383-y, 2015.

Roik, A., Röthig, T., Roder, C., Ziegler, M., Kremb, S. G. and Voolstra, C. R.: Year-Long Monitoring of Physico-Chemical and Biological Variables Provide a Comparative Baseline of Coral Reef Functioning in the Central Red Sea, PLOS ONE, 11(11), e0163939, doi:10.1371/journal. pone.0163939, 2016.

Sawall, Y. and Al-Sofyani, A.: Biology of Red Sea Corals: Metabolism, Reproduction, Acclimatization, and Adaptation, in The Red Sea, edited by N. M. A. Rasul and I. C. F. Stewart, pp. 487–509, Springer Berlin Heidelberg. [online] Available from: http://link.springer.com/chapter/10.1007/978-3-662-45201-1_28 (Accessed 7 April 2015), 2015.

Sawall, Y., Al-Sofyani, A., Hohn, S., Banguera-Hinestroza, E., Voolstra, C. R. and Wahl, M.: Extensive phenotypic plasticity of a Red Sea coral over a strong latitudinal temperature gradient

837 suggests limited acclimatization potential to warming, Sci. Rep., 5, 8940,
838 doi:10.1038/srep08940, 2015.

839 Schmidt, G. M. and Richter, C.: Coral Growth and Bioerosion of Porites lutea in Response to
840 Large Amplitude Internal Waves, PLoS ONE, 8(12), e73236, doi:10.1371/journal.pone.0073236,
841 2013.

842 Schneider, K. and Erez, J.: The effect of carbonate chemistry on calcification and photosynthesis
843 in the hermatypic coral Acropora eurystoma, Limnol. Oceanogr., 51(3), 1284–1293, 2006.

844 Schuhmacher, H., Loch, K., Loch, W. and See, W. R.: The aftermath of coral bleaching on a
845 Maldivian reef—a quantitative study, Facies, 51(1–4), 80–92, doi:10.1007/s10347-005-0020-6,
846 2005.

847 Sheppard, C. and Loughland, R.: Coral mortality and recovery in response to increasing
848 temperature in the southern Arabian Gulf, Aquat. Ecosyst. Health Manag., 5(4), 395–402,
849 doi:10.1080/14634980290002020, 2002.

850 Silbiger, N. J., Guadayol, O., Thomas, F. I. M. and Donahue, M. J.: Reefs shift from net
851 accretion to net erosion along a natural environmental gradient, Mar. Ecol. Prog. Ser., 515, 33–
852 44, doi:10.3354/meps10999, 2014.

853 Silverman, J., Lazar, B. and Erez, J.: Community metabolism of a coral reef exposed to naturally
854 varying dissolved inorganic nutrient loads, Biogeochemistry, 84(1), 67–82, doi:10.1007/s10533-
855 007-9075-5, 2007.

856 Steiner, Z., Erez, J., Shemesh, A., Yam, R., Katz, A. and Lazar, B.: Basin-scale estimates of
857 pelagic and coral reef calcification in the Red Sea and Western Indian Ocean, Proc. Natl. Acad.
858 Sci., 1414323111, doi:10.1073/pnas.1414323111, 2014.

859 Tambutté, S., Holcomb, M., Ferrier-Pagès, C., Reynaud, S., Tambutté, É., Zoccola, D. and
860 Allemand, D.: Coral biomineralization: From the gene to the environment, J. Exp. Mar. Biol.
861 Ecol., 408(1–2), 58–78, doi:10.1016/j.jembe.2011.07.026, 2011.

862 Tribollet, A. and Golubic, S.: Cross-shelf differences in the pattern and pace of bioerosion of
863 experimental carbonate substrates exposed for 3 years on the northern Great Barrier Reef,
864 Australia, Coral Reefs, 24(3), 422–434, doi:10.1007/s00338-005-0003-7, 2005.

865 Tribollet, A., Decherf, G., Hutchings, P. and Peyrot-Clausade, M.: Large-scale spatial variability
866 in bioerosion of experimental coral substrates on the Great Barrier Reef (Australia): importance
867 of microborers, Coral Reefs, 21(4), 424–432, doi:10.1007/s00338-002-0267-0, 2002.

868 Tribollet, A., Godinot, C., Atkinson, M. and Langdon, C.: Effects of elevated pCO2 on
869 dissolution of coral carbonates by microbial euendoliths, Glob. Biogeochem. Cycles, 23(3),
870 doi:10.1029/2008GB003286, 2009.

871 Uthicke, S., Furnas, M. and Lønborg, C.: Coral Reefs on the Edge? Carbon Chemistry on Inshore
872 Reefs of the Great Barrier Reef, PLoS ONE, 9(10), e109092, doi:10.1371/journal.pone.0109092,
873 2014.

874 Vaquer-Sunyer, R. and Duarte, C. M.: Thresholds of hypoxia for marine biodiversity, Proc. Natl.
875 Acad. Sci., 105(40), 15452–15457, doi:10.1073/pnas.0803833105, 2008.

876 Waldbusser, G. G., Hales, B. and Haley, B. A.: Calcium carbonate saturation state: on myths and
877 this or that stories, ICES J. Mar. Sci. J. Cons., 73(3), 563–568, doi:10.1093/icesjms/fsv174,
878 2016.

879 Wickham, H. and Chang, W.: ggplot2: An Implementation of the Grammar of Graphics. [online]
880 Available from: http://cran.r-project.org/web/packages/ggplot2/index.html (Accessed 25 June
881 2015), 2015.

882 Wiedenmann, J., D'Angelo, C., Smith, E. G., Hunt, A. N., Legiret, F.-E., Postle, A. D. and
883 Achterberg, E. P.: Nutrient enrichment can increase the susceptibility of reef corals to bleaching,
884 Nat. Clim. Change, 3(2), 160–164, doi:10.1038/nclimate1661, 2013.

885 Yeakel, K. L., Andersson, A. J., Bates, N. R., Noyes, T. J., Collins, A. and Garley, R.: Shifts in
886 coral reef biogeochemistry and resulting acidification linked to offshore productivity, Proc. Natl.
887 Acad. Sci., 112(47), 14512–14517, doi:10.1073/pnas.1507021112, 2015.

888 Zundelevich, A., Lazar, B. and Ilan, M.: Chemical versus mechanical bioerosion of coral reefs
889 by boring sponges - lessons from Pione cf. vastifica, J. Exp. Biol., 210(1), 91–96,
890 doi:10.1242/jeb.02627, 2007.

891

Tables

Table 1. Abiotic parameters relevant for reef growth at coral reef sites along a cross-shelf gradient in the central Red Sea. Temperature (Temp) and pH were continuously measured using *in situ* probes (CTDs). Weekly collected seawater samples were used for the determination of inorganic nutrient concentrations, i.e. nitrate and nitrite (NO_3^-&NO_2^-), ammonia (NH_4^+), and phosphate (PO_4^{3-}). Carbonate chemistry parameters were measured as total alkalinity (A_T) and pH in the same samples and used to calculate the carbonate ion concentration (CO_3^{2-}), aragonite saturation state (Ω_a), total inorganic carbon (C_T), bicarbonate ion (HCO_3^-), and partial pressure of carbon dioxide (pCO_2).

	Continuous data		Seawater samples									
Site / Season	**Temp**	**pH_{CTD}**	**NO_3^- &NO_2^-**	**NH_4^+**	**PO_4^{3-}**	**pH_{SWS}**	**A_T**	**HCO_3^{-*}**	**CO_3^{2-*}**	**Ωa^***	**C_T^***	**pCO_2 ***
	°C		**µmol L^{-1}**	**µmol L^{-1}**	**µmol L^{-1}**		**µmol L^{-1}**	**µmol kg^{-1}**	**µmol kg^{-1}**		**µmol kg^{-1}**	**µatm**
Avg. winter	26.0 (0.6)	8.13 (0.19)	0.36 (0.25)	0.35 (0.2)	0.07 (0.02)	8.16 (0.02)	2423 (18)	1683 (24)	299 (7)	4.62 (0.12)	1990 (21)	292 (14)
Avg. summer	31.0 (0.7)	8.15 (0.19)	0.61 (0.25)	0.5 (0.22)	0.03 (0.02)	8.13 (0.03)	2369 (38)	1588 (41)	314 (17)	4.95 (0.28)	1910 (36)	303 (25)
Nearshore exposed / winter	26.1 (0.7)	8.25 (0.27)	0.31 (0.17)	0.34 (0.19)	0.06 (0.02)	8.15 (0.02)	2414 (21)	1678 (36)	297 (6)	4.6 (0.11)	1983 (31)	295 (16)
Nearshore exposed / summer	31.5 (0.6)	8.31 (0.12)	0.6 (0.28)	0.42 (0.17)	0.02 (0.01)	8.11 (0.03)	2346 (31)	1576 (37)	309 (14)	4.88 (0.23)	1892 (32)	311 (22)
Midshore sheltered / winter	25.9 (0.6)	8.00 (0.17)	0.41 (0.31)	0.46 (0.28)	0.07 (0.02)	8.15 (0.02)	2421 (21)	1695 (19)	294 (10)	4.54 (0.14)	1997 (16)	301 (17)
Midshore sheltered / summer	30.9 (0.6)	8.09 (0.22)	0.68 (0.26)	0.58 (0.28)	0.04 (0.03)	8.11 (0.03)	2365 (40)	1603 (47)	306 (18)	4.83 (0.29)	1917 (40)	315 (31)
Midshore exposed / winter	26.1 (0.5)	8.15 (0.07)	0.32 (0.3)	0.34 (0.19)	0.06 (0.02)	8.17 (0.02)	2431 (14)	1679 (27)	304 (8)	4.7 (0.13)	1991 (21)	286 (15)
Midshore exposed / summer	30.7 (0.7)	8.16 (0.09)	0.58 (0.26)	0.5 (0.26)	0.02 (0.01)	8.13 (0.02)	2373 (38)	1594 (37)	313 (15)	4.93 (0.24)	1915 (34)	300 (16)
Offshore exposed / winter	26.0 (0.4)	8.10 (0.05)	0.4 (0.24)	0.26 (0.15)	0.08 (0.02)	8.16 (0.01)	2425 (20)	1679 (18)	302 (2)	4.66 (0.03)	1988 (19)	285 (5)
Offshore exposed / summer	30.8 (0.7)	8.12 (0.08)	0.59 (0.25)	0.51 (0.18)	0.03 (0.03)	8.15 (0.02)	2393 (35)	1579 (47)	328 (16)	5.17 (0.26)	1914 (39)	283 (19)

All values as mean (SD); pH_{CTD} = pH from CTD; pH_{SWS} = pH from seawater samples [#] day-time measurements (7:00 – 19:00); * parameters calculated using *seacarb* implemented in R (Gattuso et al., 2015; R Core Team, 2013)

905 **Table 2. Net-accretion/erosion rates G_{net} in coral reefs along a cross-shelf gradient in the**
906 **central Red Sea, cumulative over 6, 12, and 30 months.** G_{net} (kg m^{-2} yr^{-1}) was calculated using
907 weight gain/loss of limestone blocks deployed in the reef sites for 6, 12, and 30 months. Means
908 per reef site and standard deviations in brackets. yr = year

G_{net} (kg m^{-2} yr^{-1})	Deployment time (months)		
Reef site	**6**	**12**	**30**
Nearshore sheltered	0.16 (0.09)	-0.2 (0.35)	-
Nearshore exposed	0.11 (0.07)	-0.61 (0.49)	-0.96 (0.75)
Midshore sheltered	0.13 (0.09)	0.06 (0.03)	-0.29 (0.12)
Midshore exposed	0.11 (0.16)	0.01 (0.07)	0.06 (0.12)
Offshore sheltered	0.03 (0.02)	-0.07 (0.07)	-
Offshore exposed	0.14 (0.11)	0.08 (0.09)	0.37 (0.08)

909

Table 3. Reef carbonate budget estimates and contributing biotic variables (kg m^{-2} yr^{-1}) along a cross-shelf gradient in the central Red Sea. Calcification rates of benthic calcifiers ($G_{benthos}$), net-accretion/erosion rates of reef substrate ($G_{netbenthos}$), and the erosion rates of echinoids and parrotfishes (E_{echino}, E_{parrot}) contribute to the total carbonate budget (G_{budget}) in a reef site. Means per site are shown and standard deviations are in brackets. The last row gives the means and standard deviations across all sites.

Reef	G_{budget}	$G_{benthos}$	$G_{netbenthos}$	E_{echino}	E_{parrot}
Nearshore exposed	-1.477 (1.748)	0.426 (0.149)	-0.315 (0.129)	-0.228 (0.189)	-1.36 (1.886)
Midshore sheltered	0.598 (0.368)	1.15 (0.222)	-0.027 (0.014)	-0.187 (0.193)	-0.338 (0.271)
Midshore exposed	1.02 (0.353)	1.762 (0.242)	0.009 (0.003)	-0.024 (0.04)	-0.727 (0.307)
Offshore exposed	2.443 (1.033)	2.812 (0.646)	0.094 (0.022)	-0.019 (0.003)	-0.444 (0.701)
Cross-shelf gradient	0.646 (1.734)	1.538 (0.958)	-0.06 (0.168)	-0.114 (0.159)	-0.717 (1.04)

Table 4. Coefficients from Spearman rank order correlations for predictor variables vs. G_{net} and G_{budget}. 12 abiotic and 13 biotic variables were correlated with G_{net} (= net-accretion/erosion rates of limestone blocks) and G_{budget} (= carbonate budget estimates). Biotic variables encompassed the abundances of bioeroders (echinoids, parrotfishes), and 11 relevant benthic categories (%-cover). Correlates only shown, when Spearman's correlation coefficient $\rho \geq |0.59|$.

	G_{net}		G_{budget}	
Abiotic variables	**ρ**	***p***	**ρ**	***p***
Temperature(ctd) mean	-0.65	< 0.05	-0.71	< 0.05
Temperature(ctd) SD	-0.65	< 0.05	-0.71	< 0.05
pH(ctd) SD	-0.59	< 0.05	-0.65	< 0.05
A_T mean	0.80	< 0.05	0.89	< 0.05
Ωa mean	0.59	< 0.05	0.65	< 0.05
CO_3^{2} mean	0.59	< 0.05	0.65	< 0.05
PO_4^{3-}mean	0.65	< 0.05	0.71	< 0.05
Biotic variables	**ρ**	***p***	**ρ**	***p***
Rugosity	-	-	0.67	< 0.05
% total hard coral	-	-	0.70	< 0.05
% calcareous crusts	0.59	< 0.05	0.69	< 0.05

925 **Table 5. Distance based linear models (DistLM) and sequential tests.** Response variables
926 were G_{net} (net-accretion/erosion rates of limestone blocks) and G_{budget} (reef carbonate budget
927 estimates). Predictor variables were 12 abiotic variables, bioeroder abundances (one variable for
928 G_{net}, two for G_{budget}), and %-cover of relevant benthic categories (one for G_{net}, 11 for G_{budget}).
929 Significant predictors in **bold**.

Response variable: G_{net}							
Best Model	**Adj R^2**	**R^2**	**RSS**	**# of fitted Variables**			
	0.56	0.59	3.21	2			
Sequential test							
Variable	**Cumul. Adj R^2**	**SS (trace)**	**Pseudo-F**	***p***	**R^2.**	**Cumul. R^2**	**res.df**
+A_T mean	**0.54**	**4.39**	**37.84**	**0.00**	**0.56**	**0.56**	**30**
+ Ωa mean	0.56	0.27	2.48	0.12	0.03	0.59	29
Response variables: G_{budget}							
Best Model	**Adj R^2**	**R^2**	**RSS**	**# of fitted Variables**			
	0.87	0.9	6.67	6			
Sequential test							
Variable	**Cumul. Adj. R^2**	**SS (trace)**	**Pseudo-*F***	***p***	**R^2**	**Cumul. R^2**	**res.df**
+A_T (mean)	**0.65**	**46.18**	**44.13**	**0.000**	**0.67**	**0.67**	**22**
+Parrotfish abundance	**0.82**	**11.75**	**21.89**	**0.000**	**0.17**	**0.84**	**21**
+ NO3-&NO2- (mean)	0.84	1.67	3.48	0.078	0.02	0.86	20
+% encrusting coral	0.85	1.27	2.89	0.102	0.02	0.88	19
+% hard coral	0.86	0.80	1.91	0.181	0.01	0.89	18
+% Acroporidae	0.87	0.86	2.19	0.154	0.01	0.90	17

930 Cumul. Adj. R^2 = Cumulative adjusted R^2, Cumul. R^2 = Cumulative R^2, res.df = residual degrees
931 of freedom, A_T = total alkalinity

Table 6. Global comparison of the carbonate system for coral reefs.

	A_T (µmol kg^{-1})	Ω_a	pCO_2 (µatm)
Central Red Sea (this study)[1]	2346 – 2431	4.5 - 5.2	283 – 315
Global pre-industrial values (Manzello et al., 2008)[2]	~2315	~4.3	~280
Great Barrier Reef (Uthicke et al., 2014)[3]	2069 – 2315	2.6 - 3.8	340 - 554
Puerto Rico, Caribbean (Gray et al., 2012)[4]	2223 - 2315	3.4– 3.9	356 – 460
Bermuda (Yeakel et al., 2015)[5]	2300 – 2400	2.7 - 3.6	300 -450
Panama, upwelling sites (Manzello et al., 2008)[2]	1869.5	2.96	368
Galapagos (Manzello et al., 2008)[2]	2299	2.49	636

[1] lowest and highest means per reef site and season; [2] estimated averages, for details see referenced study; [3] lowest and highest means from reef sites during wet and dry seasons; [4] lowest and highest seasonal means from one site; [5] minimum and maximum from time series plots

Figures

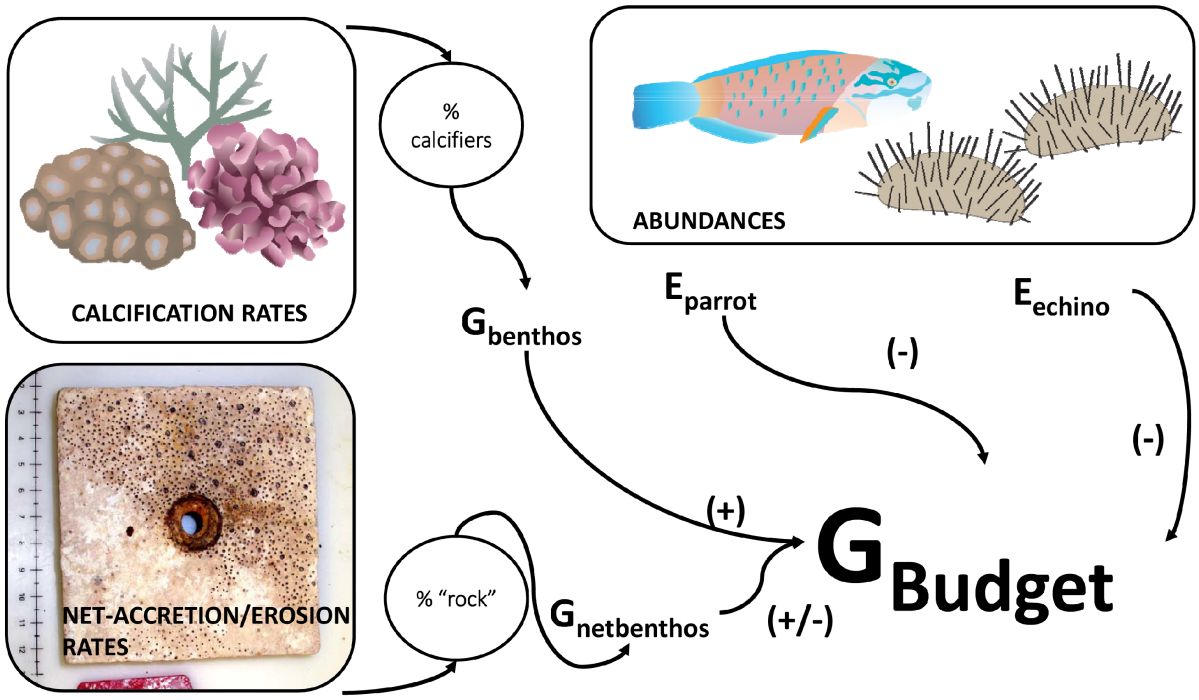

Figure 1. Schematic overview of the census based *ReefBudget* carbonate budget (G_{budget}) approach (adapted from Perry et al., 2012). Values and equations that were used are available as Supplementary Materials. $G_{benthos}$ = benthic community calcification rate, $G_{netbenthos}$ = net-accretion/erosion rate of bare reef substrate, E_{parrot} = parrotfish erosion rate, E_{echino} = echinoid (sea urchin) erosion rate, G_{budget} = carbonate budget of a reef. Images from www.ian.umces.edu.

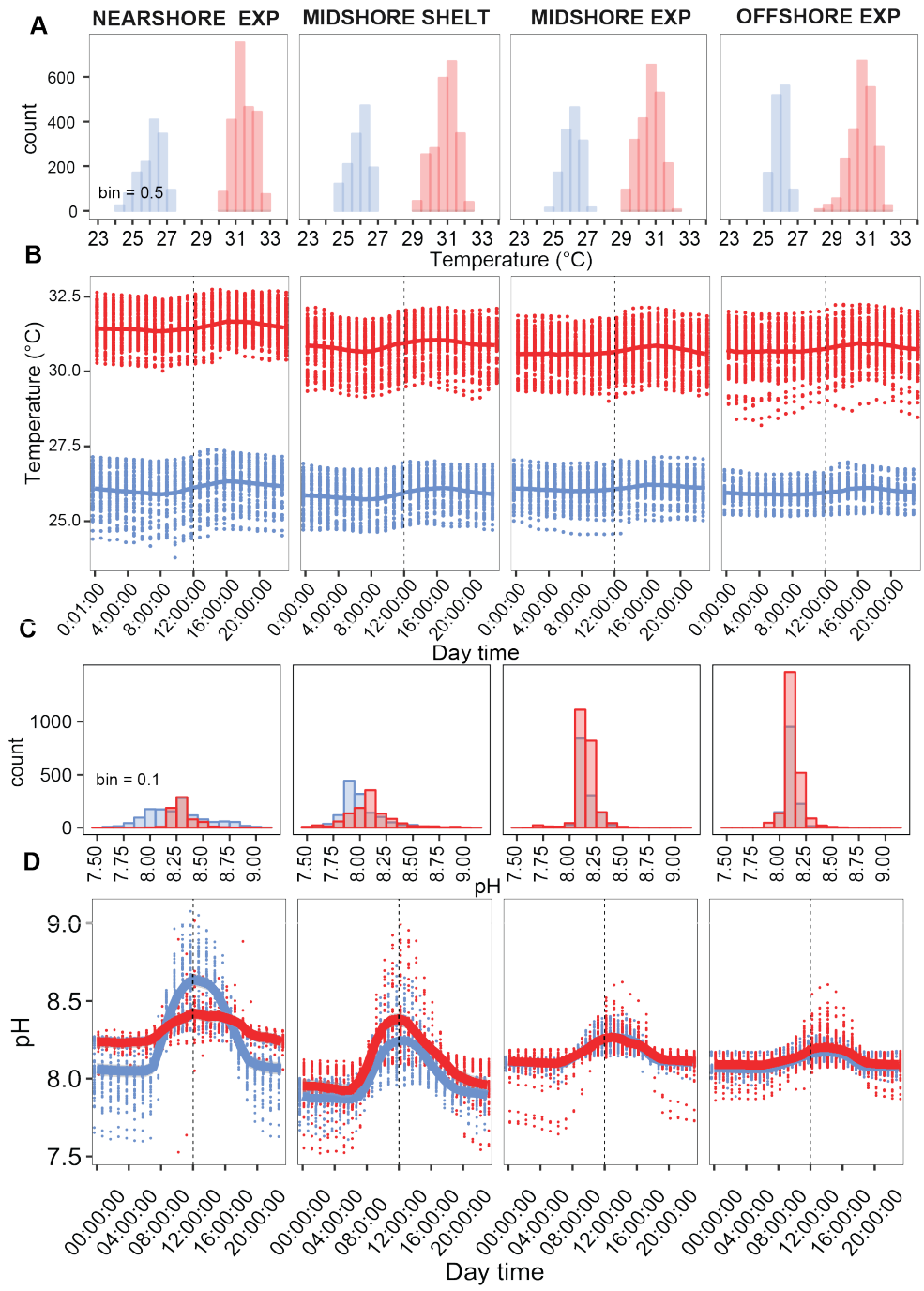

Figure 2. Seasonal temperature and pH regimes on coral reefs along a cross-shelf gradient in the central Red Sea. Continuous data of temperature (A - B) and pH_{CTD} (C - D) collected during winter (blue) and summer (red) at 0.5 m above the reef are presented in histograms (A, C) and diel profiles (B, D). Data points per reef site in winter comprise n = 1287 - 1344, and n = 1099 - 2231 in summer (nearshore summer n = 644). Diel profiles show raw data points and local polynomial regression lines (LOESS, span = 0.1). A dotted vertical line marks the midday time. EXP = exposed, SHELT = sheltered, univar. = univariate, n.s. = not significant, SD = standard deviation, min = minimum, max = maximum

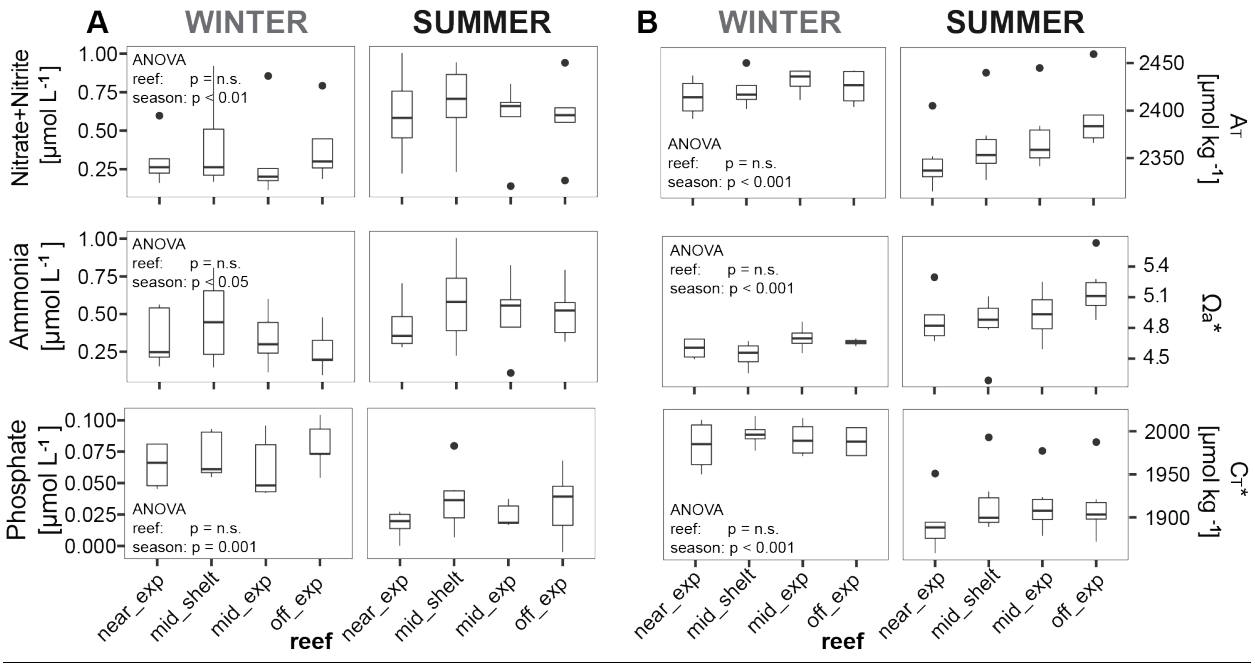

Figure 3. Inorganic nutrients and carbonate system conditions across reef sites and seasons in the central Red Sea. Boxplots illustrate the differences of seawater parameters between the reefs within each season (box: 1st and 3rd quartiles, whiskers: 1.5-fold inter-quartile range, points: data beyond this range). A_T = total alkalinity, Ω_a = aragonite saturation state, C_T = total inorganic carbon; off = offshore, mid = midshore, near = nearshore, exp = exposed forereef, shelt = sheltered lagoon, n.s. = not significant

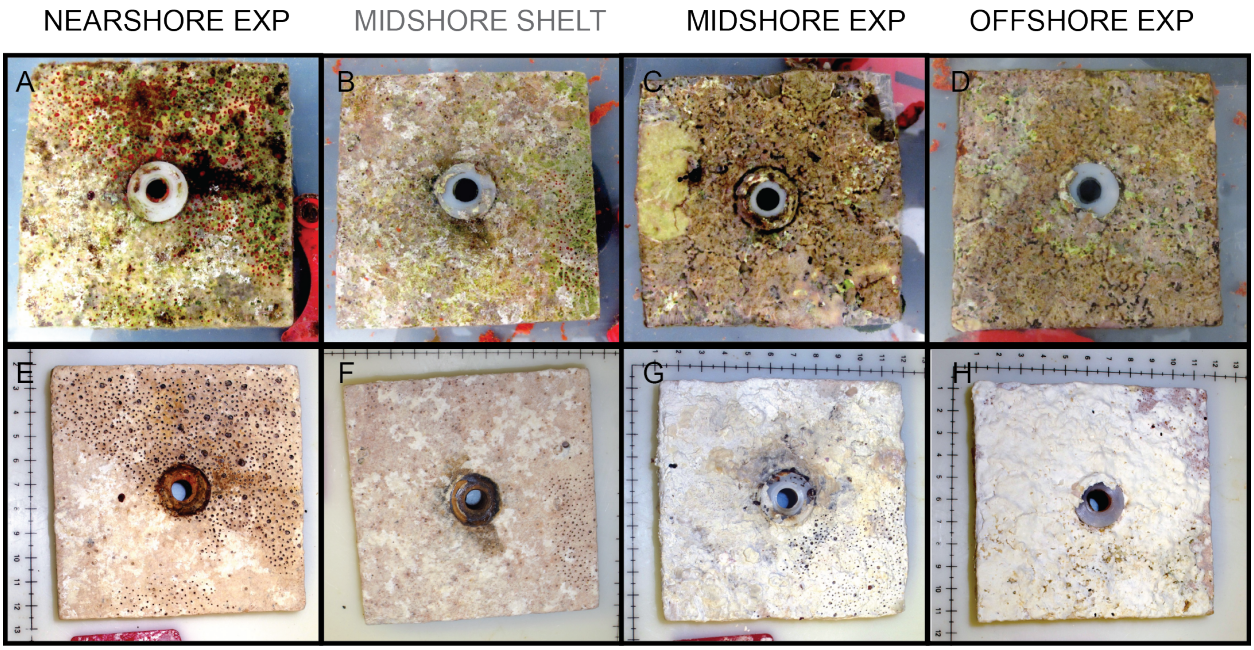

962

963 **Figure 4. Limestone blocks after 30 months of deployment in the reef sites for**
964 **measurements of net-accretion/erosion rates G_{net}.** A – D show freshly collected limestone
965 blocks that were recovered after 30 months, and the same blocks (E – H) after bleaching and
966 drying. Boring holes of endolithic sponges are clearly visible in the nearshore exposed and both
967 midshore reef sites. In the midshore and offshore exposed reefs, blocks were covered with crusts
968 of biogenic carbonate mostly accreted by coralline algae assemblages. EXP = exposed, SHELT =
969 sheltered, scales in E – H in cm.

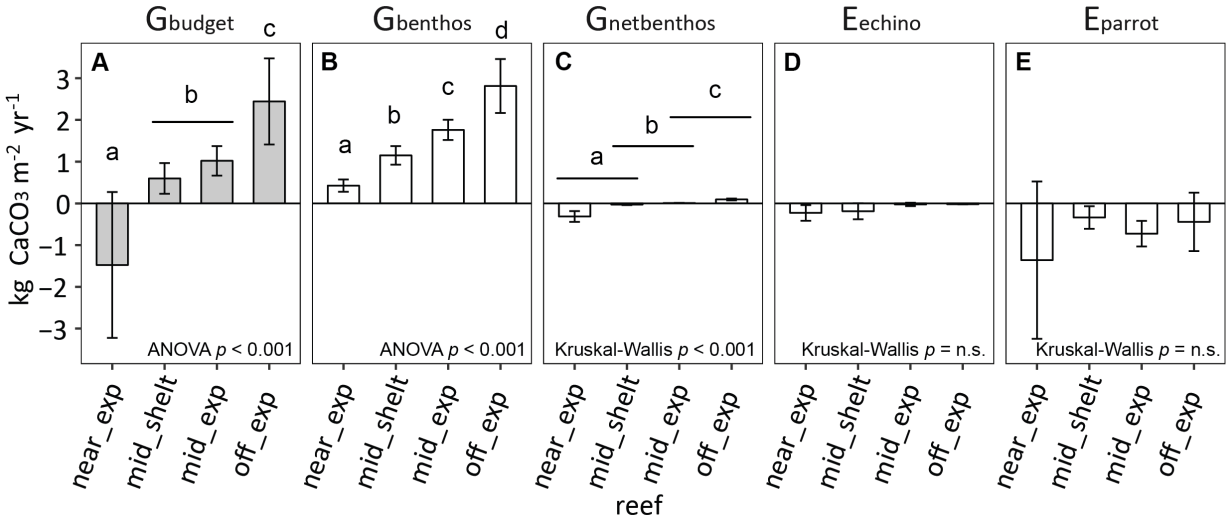

970

971 **Figure 5. Reef carbonate budget estimates and contributing biotic variables along a cross-**
972 **shelf gradient in the central Red Sea.** Benthos accretion (**$G_{benthos}$, $G_{netbenthos}$**), and the erosion
973 rates of echinoids and parrotfishes (E_{echino}, E_{parrot}) contribute to the total reef carbonate budget
974 (G_{budget}) at each reef site. All data are presented as mean ± standard deviation. (A) G_{budget} and (B
975 – E) biotic variables ($G_{benthos}$, $G_{netbenthos}$, E_{echino}, E_{parrot}). Letters a – d indicate significant
976 differences between the sites. Near_exp = nearshore exposed, mid_shelt = midshore sheltered
977 (lagoon), mid_exp = midshore exposed, off_exp = offshore exposed.